Production of the plant hormone gibberellin by rhizobia increases host legume nodule size

Ryan S. Nett[1], Kelly S. Bender[2], Reuben J. Peters[1,*]

[1]*Roy J. Carver Department of Biochemistry, Biophysics, and Molecular Biology, Iowa State University, Ames, IA 50011, USA*
[2]*Department of Microbiology, Southern Illinois University, Carbondale, IL, USA*
**Corresponding author: rjpeters@iastate.edu*

ABSTRACT

Plant-associated microbes have evolved the ability to independently produce gibberellin (GA) phytohormones as a mechanism to influence their host. Indeed, GA was first discovered as a metabolite from the fungal rice pathogen *Gibberella fujikuroi*, which uses it as a virulence factor. Though some bacterial plant pathogens similarly use GA to promote infection, symbiotic nitrogen-fixing bacteria (rhizobia), which inhabit the root nodules of legumes, also can produce GA, suggesting a role in symbiosis. The bacterial GA biosynthetic operon has been identified, but in rhizobia this typically no longer encodes the final metabolic gene (*cyp115*), so that these symbionts can only produce the penultimate intermediate GA_9. Here, we demonstrate that soybean (*Glycine max*) expresses functional GA 3-oxidases (GA3ox) within its nodules, which have the capability to convert GA_9 produced by the enclosed rhizobial symbiont *Bradyrhizobium diazoefficiens* to bioactive GA_4. This rhizobia-derived GA is demonstrated to cause an increase in nodule size and decrease in the number of nodules. The increase in individual nodule size correlates to greater numbers of bacterial progeny within a nodule, thereby providing a selective advantage to rhizobia

that produce GA during the rhizobia-legume symbiosis. The expression of GA3ox in nodules and resultant nodulation effects of the GA product suggests that soybean has co-opted control of bioactive GA production, and thus nodule size, for its own benefit. Thus, our results suggest rhizobial GA biosynthesis has coevolved with host plant metabolism for cooperative production of a phytohormone that influences nodulation in a mutually beneficial manner.

INTRODUCTION

Bacterial fixation of atmospheric nitrogen (N_2) is the major natural means by which nitrogen is assimilated into the biological environment [1]. Perhaps most relevant to agriculture is the reduction of N_2 by rhizobia, which form symbiotic relationships with legumes, including important crops like soybean (*Glycine max*), cowpea (*Vigna unguiculata*), and common bean (*Phaseolus vulgaris*), resulting in around 200 million tons of fixed nitrogen each year [2]. In this symbiosis, rhizobia reside in organs attached to the plant root called nodules, within which they are provided with a carbon source and a largely competition-free niche in exchange for their production of reduced nitrogen [3].

When inside the nodule, the rhizobia cells assume specialized, nitrogen-fixing forms referred to as bacteroids, and are located within plant nodule cells in membrane-bound symbiosomes [4]. Although the rhizobia-legume symbiosis can be considered to be mutually beneficial for each organism, both the plant and the rhizobium are working to optimize their own cost/benefit ratio within this interaction [5]. This includes rhizobia trying to “cheat” by fixing nitrogen at a sub-optimal level, which is in turn countered by host plant sanctions on these cheaters that affect rhizobial proliferation in the nodule [6]. Additionally, certain legumes can induce the

differentiation of symbiotic bacteroids into larger, branched cells. Though this seems to result in a higher symbiotic efficiency for the plant [7], it also results in a decreased ability for the rhizobial bacteroids to revert to a free-living form upon release into the soil [8]. Overall, the active competition between rhizobia and legumes to optimize their own fitness within this intimate relationship incentivizes the development of evolutionary innovations to influence the biology of their symbiotic partner. These strategies must not only specifically modulate the other organism, but also do so without inducing effects that overwhelm the advantage gained through symbiosis.

A prominent mechanism by which microorganisms commonly effect changes in plants is through the production of phytohormones [9]. Indeed, rhizobia have long been reported to produce the plant hormone gibberellin (GA) [10], and this metabolic capacity has been confirmed through characterization of GA biosynthesis in these organisms [11–15]. The ability to produce GA is imparted by a cytochrome P450 (CYP)-rich biosynthetic gene cluster referred to as the GA operon (**Figure 1**), which is widely distributed in rhizobia, but not universally present [16–18]. Transcriptomic and proteomic studies from several rhizobia species have shown that the GA operon is expressed specifically during symbiosis [19–28]. Symbiotic expression is further evident due to the presence of NifA and RpoN binding sites upstream of the operon [17, 21], both of which are involved in transcription of symbiosis-related genes in rhizobia [29], and seem to control expression of the GA operon [21]. The conditional expression of GA, as well as the crucial role of GA as a plant signaling molecule, strongly suggests that bacterial GA is playing a role within the rhizobia-legume symbiosis. Plant-synthesized GA has been demonstrated to be crucial for nodule organogenesis and development, but this hormone activity is critically dependent on timing, location, and concentration [30–34]. For example, both high or low levels of GA can result in decreased nodulation and aberrant nodule morphology [30], and thus an obvious role for rhizobial

GA in this symbiosis was not immediately apparent. Previous work has shown that bioactive GA acts as virulence factor for not only the fungal rice pathogen *Gibberella fujikuroi* (anamorph *Fusarium fujikuroi*) [35, 36], but also the rice bacterial pathogen *Xanthomonas oryzae* where the bacterial GA operon also is present [37]. By contrast, the GA operons in rhizobia typically (although not invariably), no longer contain a full-length copy of the final gene (*cyp115*) required for production of bioactive GA_4 [15, 18], such that these only produce the penultimate precursor GA_9 [12, 13]. Fragments of the *cyp115* gene that lack a full CYP catalytic domain can be found at the 5' end of some rhizobial GA operons, such as the operon found in *B. diazoefficiens* (**Figure 1**), which suggests that this gene has been selectively lost from the operon in many species of rhizobia [18]. Although GA_9 has not been found to exhibit the archetypical GA hormonal activity [38–40], the apparent production of this GA by most rhizobia suggests that it may nevertheless directly affect nodulation.

Initial analysis of the GA operon from the USDA 110 strain of *Bradyrhizobium diazoefficiens* (previously *B. japonicum*) in symbiosis with soybean found no differences in soybean height or nodulation phenotypes when plants were inoculated with either wild-type or GA operon knockout strains [41]. Although it was not yet known that this gene cluster was responsible for GA biosynthesis, this negative result suggested that the GA operon did not have an obvious effect on plant growth or nodulation. However, this experiment analyzed soybean growth and nodulation phenotypes relatively early in development (~5 weeks after planting and inoculation with rhizobia). While expression of the GA operon in bacteroids is detectable as early as 3 weeks post-inoculation [19], its expression increases noticeably during the flowering and early pod stages of soybean plant growth, suggesting that GA may have a more prominent effect later in development [12]. Consistently, GA biosynthetic activity could be detected within *B.*

diazoefficiens bacteroids isolated from nodules at the flowering and early pod stage of soybean growth, but not with bacteroids isolated during earlier stages of symbiosis [12]. Collectively, these data suggest that rhizobial GA may not have an effect until relatively late in this symbiotic relationship, as significant amounts of rhizobial GA may not be produced until the flowering stage of the plant host. Therefore a phenotype resulting from this GA production may not be evident until this point in soybean development.

Previous work reported that GA production by *Mesorhizobium loti* decreases nodule formation by its host legume *Lotus japonicus*, and further hypothesized that this restriction of nodulation provides a selective advantage by somehow excluding other rhizobia from forming symbiosis with the host plant [14]. However, increases in nodule size were also observed in this study, which could provide a more direct selective advantage, as larger nodules typically accommodate more bacterial symbionts. In addition, *M. loti* contains a functional copy of *cyp115*, and thus can produce bioactive GA_4 directly [15]. By contrast, the soybean symbiont *B. diazoefficiens* does not contain *cyp115,* and thus is only capable of producing GA_9. Here, we shown that soybean exhibits nodule-specific expression of functional GA 3-oxidase (GA3ox) homologs, which can convert GA_9 to GA_4, suggesting cooperative production of this bioactive GA phytohormone. We further demonstrated that GA produced by *B. diazoefficiens* in symbiosis with soybean increases nodule size and decreases nodule number. This increase in nodule size results in an increase in total bacteroids per nodule, and presumably a larger number of bacteria released into the soil upon nodule senescence, thereby providing a selective advantage for the GA-producing rhizobia. We hypothesize that plant expression of GA3ox in nodules may have driven the observed loss of *cyp115* in most rhizobia, enabling the host legume to optimize nodule size for

its own benefit. Thus, it appears that the biosynthesis and phenotypic effects of bacterial GA have been strongly influenced by the intricate coevolution between rhizobia and their leguminous hosts.

MATERIALS AND METHODS

Bacterial growth

See **Supplementary Table 1** for all bacterial strains used in this study. For cloning, *E. coli* strains were grown in NZY (10 g L^{-1} casein hydrolysate, 5 g L^{-1} yeast extract, 5 g L^{-1} NaCl, 1 g L^{-1} $MgSO_4 \cdot 7H_2O$) media at 37 ˚C, with 225 RPM shaking for liquid cultures. For general antibiotic use with all bacterial strains, the following concentrations were used unless stated otherwise: chloramphenicol (Cm) 25 µg mL^{-1}, kanamycin (Km) 50 µg mL^{-1}, and carbenicillin (Cb) 50 µg mL^{-1}.

B. diazoefficiens strains were grown using arabinose-gluconate (AG) media (1 g L^{-1} arabinose, 1 g L^{-1} sodium gluconate, and 1 g L^{-1} yeast extract, pH 7) with Cm at 34 µg mL^{-1}. The appropriate antibiotics to select for knockouts and/or complementing plasmids were applied as needed. For liquid cultures of *B. diazoefficiens*, 10 mL of the following sterilized supplements were added per 930 mL of AG media (making 1 L total) following autoclaving of media: HEPES-MES buffer (13 g L^{-1} HEPES, 11 g L^{-1} MES, pH 6.6-6.9), 0.67 g L^{-1} $FeCl_3$, 18.0 g L^{-1} $MgSO_4 \cdot 7H_20$, 1.3 g L^{-1} $CaCl_2 \cdot 2H_20$, 25.0 g L^{-1} $NaSO_4$, 32.0 g L^{-1} NH_4Cl, and 12.5 g L^{-1} Na_2HPO_4.

Rhizobia knockout strains

To generate a GA operon insertional knockout strain (*B. diazoefficiens* KB2011, ga^-), a 1946 bp DNA fragment corresponding to the *cyp112* gene and portions of the flanking genes (*pseudo-cyp115* and *cyp114*, **Supplementary Figure 1**) was PCR amplified from *B. diazoefficiens* USDA 110 genomic DNA (gDNA) using primers Bd-cyp112-PmeI-F and Bd-cyp112-PmeI-R (see **Supplementary Table 2** for primer sequences). The resulting fragment, which corresponded to the *B. diazoefficiens* USDA 110 genome coordinates 2317624 – 2319579, was ligated into the commercial pJET-cloning vector for further manipulation (see **Supplementary Table 3** for a list of plasmids used). The *cyp112* gene within this fragment was interrupted using an intrinsic EcoRI site (located 739 bp downstream of the *cyp112* start codon) and an EcoRI fragment from pHP45Ω [42] containing the *aadA* gene (encoding streptomycin resistance) flanked by strong terminators. This ligation resulted in a 4025 bp GA operon polar knockout cassette, which was inserted into the PmeI restriction sites of the mating/SacB counterselection vector pLO1 [43]. The resulting pLOBJ3 vector was transformed into the *E. coli* mating strain S17-1 λ *pir* for subsequent delivery to *B. diazoefficiens*.

Conjugation reactions between wild type *B. diazoefficiens* USDA 110 grown in HM medium [44] (0.125 g L^{-1} Na_2HPO_4, 0.25 g L^{-1} Na_2SO_4, 0.32 g L^{-1} NH_4Cl, 0.18 g L^{-1} $MgSO_4 \cdot 7H_2O$, 0.004 g L^{-1} $FeCl_3$, 0.013 g L^{-1} $CaCl_2 \cdot 2H_2O$, 1.3 g L^{-1} HEPES, 1.1 g L^{-1} MES; pH 6.6) supplemented with 0.1% (w/v) arabinose (no other carbon source or yeast extract) and S17-1 λ *pir* /pLOBJ3 were set up as follows: 1 ml of each culture at an OD600 of ~0.7 were mixed, pelleted, washed two times with HM medium to remove antibiotics, resuspended in 25 µL of HM, and spotted on a 0.45 µm filter placed on a HM/0.1% arabinose plate. Additional carbon sources and yeast extract were not added to promote mating between *B. diazoefficiens* and S17-1 λ *pir* as the nutrient limitation prevented exopolysaccharide production by *B. diazoefficiens*. After 3 days of incubation at 30 ºC,

159 the mating reactions were resuspended from the filter into 1 mL of HM and dilutions were plated
160 on YEM-HM medium [45] (HM medium with 0.5% [w/v] mannitol, 0.025% [w/v] yeast extract,
161 and 0.05% [w/v] L-arabinose) containing 30 µg mL^{-1} Cm to select against the donor S17-1 λ *pir*
162 (as *B. diazoefficiens* USDA 110 is naturally resistant), 100 µg mL^{-1} streptomycin (Sm) to select
163 for the *aadA* interruption cassette, and 100 µg mL^{-1} kanamycin to select for chromosomal insertion
164 of pLOBJ3 (pLOBJ3 cannot be stably maintained in *B. diazoefficiens*).

165 Transconjugants that appeared after 4-5 days were screened for integration of the pLOBJ3
166 vector into the chromosomal *cyp112* region via PCR targeting chromosomal regions outside of the
167 insertion site and regions within the unstable vector. Positive recombinants were grown up in liquid
168 YEM-HM medium with 30 µg mL^{-1} chloramphenicol and 100 µg mL^{-1} Sm for 3 days to promote
169 removal of the remaining vector (encoding SacB) from the chromosome through a second
170 recombination event between the wild type *cyp112* region and pLOBJ3.

171 The second recombination event and thus final GA operon knockout strain was counter-
172 selected for using Modified Bergersens[4] (MB) medium (0.23 g L^{-1} K_2HPO_4, 1.1 g L^{-1} sodium
173 glutamate, 0.1 g L^{-1} $MgSO_4 \cdot 7H_2O$, 1 mL ultrapure trace element stock, 1 mL vitamin stock, and 4
174 mL glycerol) containing 5% (w/v) sucrose and 100 µg mL^{-1} of Sm, as strains still containing the
175 integrated plasmid expressed SacB making them sensitive to sucrose. Sucrose resistant colonies
176 appearing after 6-10 days were also screened for sensitivity to kanamycin to verify loss of the
177 pLOBJ3 plasmid. Interruption of the GA operon was verified in sucrose sensitive, kanamycin
178 sensitive, and streptomycin resistant colonies by Southern blots hybridized with probes
179 corresponding to the *cyp112*, *aadA*, and *blr2150* (*Bd*KS; outside of the interrupted GA operon)
180 genes (**Supplementary Figure 2**). Compared to the wild type, three selected mutant strains

possessed the *aadA* interruption cassette. The insertion of the *aadA* interruption cassette resulted in the chromosomal XhoI fragment containing the *cyp112* gene to increase in size from 4010 bp (**Supplementary Figure 2c, lane 4**) to 6089 bp (**Supplementary Figure 2c**, **lanes 1-3**). Hybridization with a control probe corresponding to the downstream gene *cyp114*, which is located on a separate XhoI fragment, indicated no differences between the mutant and wild type strains (**Supplementary Figure 2d**). Further PCR analysis targeting the region spanning the *pseudo cyp115* and *cyp114* genes confirmed the interruption of the GA operon as the expected product size increased from the 2195 bp observed in the wild type to the 4275 bp in the mutants (**Supplementary Figure 3a**). This 2080 bp increase corresponded to the *aadA* interruption cassette. The PCR analysis also confirmed the removal of the pLOBJ3 interruption vector through a second recombination event as the plasmid encoded *sacB* gene was not detected in the mutants (**Supplementary Figure 3b**). In total, three GA operon knockout strain were confirmed and named *B. diazoefficiens* KB903, KB904, and KB2011. Initial PCR confirmation of the knockout insertion was more consistent in *B. diazoefficiens* KB2011, and thus this strain was selected for further experimentation.

Deletion strains for the individual CYPs within the GA operon for *B. diazoefficiens* (*Bd*Δ*cyp117*, *Bd*Δ*cyp114*) were previously developed for characterization of GA biosynthesis in rhizobia [13]. These strains were grown in AG media under aerobic growth conditions to determine if knockout of the GA operon significantly affects rhizobial growth. This demonstrated that the deletion of *cyp117* and *cyp114* did not affect aerobic rhizobial growth, while a small decrease in growth rate was observed with *B. diazoefficiens* KB2011 (**Supplementary Figure 4**), which is presumably due to the constitutive expression of the streptomycin resistance gene. Collectively, these results suggest that the GA operon does not have an effect on general rhizobial growth.

Plant growth, inoculation, measurements, and nodule harvest

Soybean (*Glycine max* cv. Williams ’82) seeds were surface sterilized for 10 minutes with 20% Clorox (6% [w/v] sodium hypochlorite) followed by five washes with sterile water. Seeds were then immersed in 0.01 M HCl for 10 minutes followed by an additional five washes with sterile water, and then germinated on sterile, moist paper towels in the dark for 3 days. After germination, seeds were planted into a 3:1 mixture (v/v) of sterile vermiculite and perlite within 4” diameter x 3.5” tall pots and were grown in a growth chamber with 16 hours of light at 27 ºC and 8 hours of darks at 18 ˚C. Plants were watered as needed with sterile, deionized water, unless otherwise noted. Once per week, the plants were supplemented with Murashige and Skoog (MS) nutrient solution (pH 5.8-6.0) without nitrogen (bioWORLD).

Plants were inoculated with rhizobia one week after planting. To do so, *B. diazoefficiens* liquid cultures (wild-type or knockout) were grown until late log phase (7-10 days), at which point cultures were centrifuged at 5000 x *g* for 10 min to pellet cells. Pellets were resuspended in an original culture volume of sterile water to wash away media and antibiotics, then centrifuged again at 5000 x *g* for 10 min. Pellets were then resuspended in sterile water to a final OD600 of 0.100 ± 0.003. For each plant, 10 mL of the appropriate rhizobial suspension was pipetted into the vermiculite/perlite soil substrate.

Vegetative stage (3 weeks post inoculation), flowering stage (~5-6 weeks post inoculation), early pod stage (~8 weeks post inoculation), full pod stage (>10 weeks post inoculation). Upon harvest, vermiculite and perlite attached to the root system was removed with light shaking and gentle washing with water. Roots were then patted dry with a paper towel. Root and green mass

measurements were taken immediately following harvest. Height measurements were taken from the cotyledon scar up to the base of the apical meristem. Note that growth was limited in large part to the height of the growth chamber in use, and thus plant height measurements beyond ~6-7 weeks of growth (at which point plants have grown up to the top of the growth chamber) are likely not representative of normal plant growth. However, the vine-like nature of *G. max* Williams '82 allowed for these plants to continue growing laterally within the growth chamber. Nodules were removed from the roots by hand, counted, and the collective total mass of the nodules was measured. Mass per nodule was calculated by dividing the total nodule mass per plant by the number of nodules. For direct comparisons between plants nodulated with GA^+ or ga^- rhizobia, statistical tests were carried out using Student's t-test within Microsoft Excel, while multiple comparisons were performed in JMP Pro 13.

Chemical complementation

For chemical complementation experiments, soybean plants were germinated, planted, and inoculated in the same manner as described above (see **Plant growth, measurements, and harvest**). After three weeks, at which point the GA operon has been implicated to be expressed [19, 23], plants were watered twice per week with 50 mL of either a GA solution or sterile water. The GA_9 solutions were made by dissolving GA_9 (provided by Dr. Peter Hedden, Rothamsted Research, Harpenden, U.K.) in methanol at stock concentration of 0.1 M. An appropriate amount of this stock (or a serial dilution of the stock) was added to sterile water to make 100 nM, 10 nM, and 1 nM solutions. Preliminary experiments with GA_9 suggested that concentrations at or below 100 nM did not have any significant effects on nodulation. As such, follow up experimentation

with GA_9 supplementation at 1 µM was performed. The GA_3 solutions were made in the same method as those for GA_9, with the exception that for the 0.1 M stock solution, GA_3 (Sigma-Aldrich) was dissolved in ethanol. Statistical analyses for chemical complementation experiments were carried out using JMP Pro 13.

While previous studies have shown that GA_3 concentrations of 1 µM are inhibitory to nodule formation, they have also observed that aberrant plant growth phenotypes such as increased height and decreased root formation are associated with concentrations greater than or equal to 10 nM [46]. A subtle, though non-significant increase in height was observed in this experiment from 10 nM GA_3, but application with concentrations of 100 nM resulted in extreme increases in height as early as one-week after such treatment was begun. Additionally, a significant reduction in root mass was observed at the higher concentrations (10 nM and 100 nM), consistent with an inhibitory effect of GA_3 on root growth. Because rhizobial GA production does not affect the overall height and mass phenotypes of the plant, it can be reasoned that rhizobia are producing GA at levels lower than those applied in these experiments. While a higher concentration of GA_9 was needed to observe a similar effect to lower levels of GA_3 (1 µM vs. 10 nM, respectively), we predict that this is due to the difference in solubility between GA_9 and GA_3 (predicted logP of 2.76 and 0.01, respectively), along with the presumed need for GA_9 to be metabolized to a bioactive form.

Bacteroid isolation and counting

Prior to homogenization, soybean nodules were washed five times with 100 µL of sterile water to remove contaminating microbes. *B. diazoefficiens* bacteroids were extracted from root nodules via grinding in ascorbate buffer (100 mM KH_2PO_4, 200 mM sodium ascorbate, 2% [w/v]

polyvinylpyrrolidone, and 34 µg mL^{-1} Cm, pH 7.5). Plant material was removed with centrifugation at 100 x *g* for 10 min. The supernatant was removed, and this fraction was then centrifuged at 5000 x *g* for 10 min. to pellet the bacteroids. Bacteroid pellets were then resuspended in 1 mL of sterile 0.85% (w/v) NaCl solution.

To determine the number of viable bacteroids, serial dilutions were created for three samples from each time point and/or condition, and 10 µL of these dilutions were plated on AG plates in triplicate. After 6-7 days of incubation at 30 ºC, colony forming units (CFUs) were counted, and total number of viable bacteria per nodule mass were calculated.

Total numbers of bacteroids extracted from nodules was measured with flow cytometry. Aliquots of isolated bacteroids from three samples per time point and/or condition were stained using the LIVE/DEAD BacLight Bacterial Viability kit (Thermo Fisher Scientific), which contains SYTO9 dye for staining live cells and propidium iodine (PI) for staining dead cells, and this was done as per the manufacturer instructions. Additionally, counting beads provided in this kit (with a known concentration) were added to each sample in order to facilitate quantification of the total number of cells in the sample. Samples were run and counted using a BD FACSAria III flow cytometer (BD Biosciences). Linear regressions for this data were plotted in Microsoft Excel, and statistical analysis was performed using JMP Pro 13.

Soybean GA 3-oxidase cloning and heterologous expression

Soybean contains eight GA 3-oxidase isoforms (GmGA3ox1-8) that are all annotated as belonging to the Fe(II)/2-oxoglutarate dependent dioxygenase (2ODD) family [47], which was expected based upon previous characterization of GA 3-oxidases. PCR screening for six of these

GA3ox (specifically, those previously described in the literature [47]) with cDNA synthesized from nodule RNA revealed that Gm*GA3ox4* (gene ID: 100780857; locus tag: Glyma14g16060) and Gm*GA3ox6* (gene ID: 100808546; locus tag: Glyma17g30800) were the only isoforms noticeably expressed in the nodule at 8 weeks post inoculation with *B. diazoefficiens*. Based on this information, *E. coli* codon-optimized synthetic clones of the coding sequences of these genes (sGm*GA3ox4* and sGm*GA3ox6*) were synthesized via GeneArt Strings synthesis (Thermo Fisher Scientific). Cloned genes were amplified with primers specific to the 5' and 3' of the ORFs, with an additionally CACC added onto the 5' primer (**Supplementary Table 2**) to allow for directional cloning into the pET101/D-TOPO (Champion pET101 Directional TOPO Expression Kit; Thermo Fisher Scientific) expression vector. The stop codon of each gene was included on the reverse primer to exclude the C-terminal His-tag encoded within pET101. Following PCR amplification with Accuprime Pfx (Thermo Fisher Scientific) and gel purification, synthetic clones were ligated into pET101/D-TOPO as per the product manual, transformed into chemically competent Top10 cells, and selected on agar plates containing carbenicillin (Cb). Positive clones were screened with colony PCR and confirmed with Sanger sequencing. This resulted in the construction of pET101-sGm*GA3ox4* and pET101-sGm*GA3ox6* expression plasmids. A negative clone of pET101 created during this process was kept and used as an empty vector control.

These plasmids were then transformed into chemically competent *E. coli* BL21-star for heterologous expression. Positive colonies were used to inoculate 5 mL terrific broth (TB) media (10 g L^{-1} casein, 24 g L^{-1} yeast, 0.4% [v/v] glycerol, pH 7) cultures, which were allowed to grow overnight. 500 µL of these cultures was then used to inoculate 50 mL TB cultures containing 5 mL of phosphate buffer (pH 7.5) and appropriate antibiotics, and these cultures were allowed to grow at 37 ºC and 225 RPM shaking until reaching an OD600 of 0.6-0.8, at which point they were

incubated for an hour at 16 ºC with 225 RPM shaking. Following this incubation, isopropyl β-D-1-thiogalactopyranoside (IPTG) was added at 1 mM to induce expression. At this time, the 2ODD cofactors 2-oxoglutarate (a.k.a α-ketoglutarate; final concentration of 4 mM), ascorbate (final concentration of 4 mM), and $FeSO_4$ (final concentration of 0.5 mM) were added, along with GA substrate (final concentration of 5 µM). Cultures were then allowed to incubate at 16 ºC with 225 RPM shaking for 3-4 days, after which point metabolites were extracted (see **Metabolite extraction and purification**). Through this process, both enzymes were verified as specifically having GA3ox activity, as in addition to C-3β hydroxylation of GA_9 to form GA_4, heterologously expressed GA3ox4 and GA3ox6 converted GA_{20} (i.e. 13-hydroxy GA_9) into GA_1, another common bioactive GA endogenous to plants, via C-3β hydroxylation.

Additionally, Gm*GA3ox6* function was characterized *in vitro* within crude cell lysates. Expression conditions were nearly identical to those described earlier, with the exception that NZY media was used instead of TB. To begin, 5 mL NZY cultures of the appropriate transformed *E. coli* BL21 strain were grown under antibiotic selection overnight, and were used to inoculate 1.0 L cultures of NZY. These were grown at 37 ºC with 225 rpm shaking to an OD600 of 0.6 to 0.8, at which point they were transferred to 16 ºC with 225 rpm shaking for 1 hour. Cultures were induced with IPTG (1 mM) and allowed to shake overnight at 16 ºC. After this incubation, cells were centrifuged at 5000 x *g* for 10 min to pellet cells, and these pellets were then resuspended in 10 mL Tris buffer (100 mM Tris-HCL, 4 mM dithiothreitol, pH 7.1). Resuspended cells were homogenized with an EmulsiFlex C-5 (Avestin, Canada) or by sonication, and cell debris was pelleted with centrifugation at 17,000 x *g* for 30 min at 4 ˚C. Cell lysates were aliquoted and reactions were set up either with or without a 2ODD supplement mixture (final concentrations of 4 mM 2-oxoglutarate, 4 mM ascorbate, 0.5 mM $FeSO_4$, 2 mg mL^{-1} bovine serum albumin, and 0.1

mg mL^{-1}). GA substrate (at 5 µM) was added to the mixtures, and these were incubated at 30 ºC for 12 hours, after which they were extracted as described below. These experiments confirmed the nature of these enzymes as 2ODDs, as activity was only detected in the presence of the necessary 2ODD cofactors α-ketoglutarate, ascorbate, and iron.

Metabolite extraction and purification

GA incubation assays (both whole cell and cell lysates) were first acidified to pH 3 with 5 M HCl in order to neutralize free carboxylates. Each incubation was then extracted three times with an equivalent volume of ethyl acetate, and these extracts were pooled in a round bottom flask and dried using a rotary evaporator. Dried extracts were washed 3 times with 3 mL fractions of ethyl acetate, which were pooled in glass tubes and dried under a gentle stream of N_2. Each extract was then purified over a silica column. This was done by first resuspending the sample in 1 mL of hexane and adding the sample to a silica column pre-washed with hexane. The column was then washed with successive 1 mL solutions of ethyl acetate in hexane, starting with 100% hexane, and increasing the ethyl acetate proportion with each wash. Collected fractions were derivatized with diazomethane at room temperature for 1 hour in order to methylate free carboxylic acids. These were dried under a gentle stream of N_2, then resuspended in either BSTFA+TMCS [*N*,*O*-Bis(trimethylsilyl)trifluoroacetamide + Trimethylchlorosilane; 99:1 v/v] or MSTFA [*N*-Methyl-*N*-(trimethylsilyl)trifluoroacetamide] and incubated at 80 ºC for 30 min in order to silylate free alcohols to the trimethylsilyl (TMS) ether. Derivatized samples were then dried under a gentle stream of N_2, and resuspended in n-hexane for gas chromatography-mass spectrometry (GC-MS) analysis.

Gas chromatography-mass spectrometry (GC-MS) analysis

Samples were run on a Varian 3900 GC equipped with an HP-5MS column (Agilent) paired with a Saturn 2100T MS detector (Varian). For each sample, 1 µL was injected under splitless mode with an initial injector temperature of 250 ˚C, column flow rate of 1.2 mL min^{-1}, and an initial column oven temperature of 50 ºC, which was held for 3 min. The column oven temperature was then increased at a rate of 15 ˚C min^{-1} until a final temperature of 300 ºC, at which point this temperature was held for 3 min. Electron ionization was used to ionize and fragment compounds, and mass spectra data with a range of 90-650 *m/*z was collected starting at 13 min and continued until the end of the run. Potential products were compared to previously published mass spectra [48], and were further confirmed via comparison to authentic standards.

RNA isolation, cDNA synthesis, and RT-qPCR

Plant tissue (root nodules and roots, each in triplicate) collected from plants harvested at 3 to 15 weeks post rhizobial inoculation were ground in liquid nitrogen with a mortar and pestle, and RNA was purified from equivalent amounts of homogenized tissue using the RNeasy Plant Mini Kit (Qiagen) as per the manufacturer's instructions. Contaminating DNA was digested and removed using the Turbo DNA-*free* kit (Life Technologies), and cDNA was synthesized using the iScript cDNA Synthesis kit (Bio-Rad) according to the manufacturer's instructions. PCR amplification using primers specific to the genes of interest was performed using RNA, DNase-treated RNA, and cDNA as templates to confirm that downstream PCR analysis was only detecting cDNA.

Quantitative reverse transcription PCR (RT-qPCR) was performed to test expression of the *cyp112* (NCBI gene ID: 1055403; locus tag: blr2144) and *ks* (NCBI gene ID: 1055399; locus tag: blr2150) genes from the GA operon in *B. diazoefficiens* USDA110, along with two GA 3-oxidase homologs (Gm*GA3ox4* and Gm*GA3ox6*) from soybean. For *B. diazoefficiens* genes, *hisS* (histidyl-tRNA synthetase; NCBI gene ID: 1054697; locus tag: bll7457) was used as the internal reference gene as previously described [20, 49]. For soybean genes, *cons7* (NCBI gene ID: 100804856; locus tag: Glyma_03g137100), which has been identified to be expressed stably under a number of conditions, including nodule development [50], was used as the reference gene (see **Supplementary Table 4** for the sequences of RT-qPCR primers used). RT-qPCR samples were prepared with PowerUp SYBR Green Master Mix (Life Technologies) according to the recommended manufacturer conditions with primers at a final concentration of 500 nM. Reactions were run and measured on a StepOnePlus thermocycler (Applied Biosystems). The following program was used for each primer set: 50 ºC for 2 minutes followed by 95 ºC for 2 minutes, then 45 cycles of 95 ºC for 15 seconds and 60 ºC for 1 minutes. After these cycles, a melt curve stage was performed to confirm specificity of the RT-qPCR reaction as per the instructions of the aforementioned RT-qPCR kit. Primer efficiencies were determined for each primer set by using serial dilutions of PCR amplified cDNA fragments generated from soybean cDNA (or fragments generated from gDNA for *B. diazoefficiens*) as template, and this analysis confirmed the reported primer sets to have between 90 and 110% efficiency (**Supplementary Figure 5**).

RESULTS

To confirm expression of the GA operon in *B. diazoefficiens* during its symbiosis with soybean, nodules were harvested over a 12-week span of soybean development (covering the

vegetative to full-pod stages) [51], and quantitative reverse transcription PCR (RT-qPCR) was used to measure the relative expression of two rhizobial GA operon genes (*cyp112* and *ks*). This analysis confirmed that the operon is expressed early in symbiosis (3 weeks post inoculation), and that expression continues throughout the flowering and early pod stages of plant development (**Supplementary Figure 6**). Because previous studies have not found any differences in plant phenotypes related to rhizobial GA during early stages of soybean development [41], and because bacteroid GA biosynthetic enzyme activities are not observed until around the soybean flowering stage [12], it was reasoned that studies of such metabolism and its effect should be focused on this stage of host plant development.

Unlike *M. loti*, the soybean symbiont *B. diazoefficiens* does not contain a functional copy of *cyp115* [13]. Thus, like most other rhizobia containing the GA operon, this species can only produce GA_9. Given that GA_9 is considered to be the penultimate precursor and does not exhibit hormonal activity on its own, as it does not elicit a response in growth assays [38] and does not bind effectively to the appropriate GA receptor [39, 40], we hypothesized that soybean might express functional GA3ox to convert the rhizobia-produced GA_9 to bioactive GA_4 in its nodules. To investigate this possibility, PCR with cDNA generated from flowering stage nodule RNA was used to probe the six GA3ox isoforms predicted within the soybean genome [47]. It was possible to detect expression of two isoforms, Gm*GA3ox4* (gene ID: 100780857) and Gm*GA3ox6* (gene ID: 100808546), suggesting that these may represent GA3ox enzymes specific to the nodule (**Supplementary Figure 7**). Subsequent RT-qPCR analysis demonstrated that transcripts for both Gm*GA3ox4* and Gm*GA3ox6* are expressed at significantly higher levels in nodules than elsewhere in the roots, and are present in the nodule throughout all stages of plant development that were assessed here (**Supplementary Figure 7**). Our results differ somewhat from previous RNA-seq

analyses of the soybean nodule [52, 53], which did not find enrichment of these genes within the nodule relative to other tissues. It is unclear why this discrepancy was observed, and future investigations into GA3ox homolog expression over the full nodule lifetime may be necessary to fully understand the potential roles of soybean GA3ox genes in this symbiosis. Regardless, our ability to detect enrichment of GA3ox homolog expression within the nodule suggests a potential role for these genes in converting rhizobial GA_9 into bioactive GA hormones.

The biochemical function of the enzymes encoded by Gm*GA3ox4* and Gm*GA3ox6* were confirmed via heterologous expression in *E. coli* (**Supplementary Figures 8, 9, & 10**). Importantly, their capability to act on the rhizobial GA product was demonstrated, as incubation of GA_9 with cells expressing either Gm*GA3ox4* or Gm*GA3ox6* resulted in 3β-hydroxylation of GA_9, thereby producing GA_4 (**Supplementary Figure 8**). This confirmed that these putative GA3ox exhibit the predicted ability to convert GA_9 into the bioactive GA_4. Although these data do not confirm *in planta* conversion of rhizobial GA_9 into GA_4, they demonstrate that functional soybean GA3ox enzymes are expressed in the correct tissue and at the appropriate time for them to act on GA_9, which is presumably secreted by bacteroids within the nodule, thereby suggesting the potential for cooperative production of bioactive GA_4 by these symbiotic partners.

To evaluate the phenotypic role that this rhizobial produced GA may be playing in symbiosis, we generated a GA operon knockout strain from the wild-type strain *B. diazoefficiens* USDA 110 (GA^+). This was accomplished by inserting an antibiotic resistance cassette into *cyp112*, resulting in the strain *B. diazoefficiens* KB2011 (ga^-), a polar knockout in which transcription of the entire GA operon was essentially eliminated (**Supplementary Figure 11**). Plants nodulated with the ga^- strain did not have significantly altered height, green tissue mass, or

root mass from plants nodulated with the GA^+ strain (**Figure 2a, b**), which agrees with previous reports showing that the GA operon does not appear to affect major growth phenotypes of the plant [14, 41]. Additionally, much like previous analysis of a GA operon knockout strain of *B. diazoefficiens* [41], no significant alterations in nodulation were observed early in soybean development (vegetative stage; 3 weeks post inoculation). However, by the soybean flowering stage (7 weeks post-inoculation) there were noticeable differences in nodulation phenotypes. In particular, plants nodulated by the ga^- strain had a significant increase in their number of nodules by this stage (**Figure 2c**). However, these nodules were on average significantly smaller than those in plants inoculated with the GA^+ strain (**Figure 2d**). These effects are particularly striking at the full pod stage (18 weeks post-inoculation), as nodules from plants inoculated by GA^+ *B. diazoefficiens* are roughly twice as large as those from plants inoculated by the ga^- strain, while the total number of nodules per plant for the ga^- strain are essentially twice that of plants inoculated with the GA^+ strain. Correspondingly, additional analysis of nodule size distribution at the full-pod time point demonstrated that knockout of the GA operon resulted in significantly fewer large nodules and an increased number of smaller nodules (**Figure 2f**).

Overall, this disparity in nodule size and number did not significantly alter the total nodule mass per plant by the early pod and full pod stages (**Figure 2e**). The similarity in total nodule mass, as well as total plant mass, suggests that knockout of the GA operon does not restrict nitrogen assimilation by the plant. However, because plants nodulated by the ga^- strain form significantly more nodules, it seems likely that the plant needs to compensate for smaller average nodule size, and correspondingly, the nitrogen fixing-capacity of each nodule. A similar effect on nodulation (i.e. an increased number of smaller nodules), with no effect on overall plant growth, was also demonstrated with two additional GA operon gene-deletion strains, *Bd*Δ*cyp117* and *Bd*Δ*cyp114*

[13], confirming that perturbation of the GA operon, and thus rhizobial GA production, is responsible for the knockout phenotypes (**Supplementary Figure 12**). While the presence of GA seems to have a clear effect on the size and number of nodules, the overall morphology and appearance of the nodules from plants inoculated with the GA^+ or ga^- strains were indistinguishable (**Supplementary Figure 13**), which suggests that nodule organogenesis occurs normally, and that rhizobial GA only affects the nodules after their establishment.

In agreement with bioactive GA being the signaling molecule associated with the observed phenotypes, application of GA_3 (a readily available bioactive GA) to the roots of plants inoculated by the ga^- strain restored wild-type levels of nodule number and average nodule size (**Figure 3**). This was evident for GA_3 concentrations as low as 1 nM, and at this lowest concentration only minimal effects on overall plant growth were observed (**Supplementary Figure 14**). By contrast, chemical complementation with GA_9, the apparent final product of GA biosynthesis by *B. diazoefficiens* [12, 13], required significantly higher concentrations (1 µM) to restore average nodule mass and nodule numbers to wild-type (GA^+) levels for plants in symbiosis with the ga^- strain (**Supplementary Figure 15**), and significant changes in average plant height and masses were observed at this concentration (**Supplementary Figure 16**). Due to the high concentrations of GA_9 required to alter the nodule size and numbers, it is unclear whether this chemical treatment is truly rescuing the GA^+ phenotype, or if this effect is simply an artefact of GA signaling throughout the roots, which could lead to a restriction in nodulation [30]. Nevertheless, the significantly lower concentrations of bioactive GA required to effect changes in nodule phenotypes for soybean inoculated with ga^- rhizobia is consistent with the phenotype being due to low levels of bioactive GA, which would require host conversion of GA_9 into GA_4.

Based upon these results we hypothesized that rhizobial GA provides a selective advantage to rhizobia through increasing nodule size. GA phytohormones are known to promote individual cell expansion during plant growth [54], and thus could signal to increase cell size within the nodule, resulting in enlarged nodules. Because larger nodules typically contain greater numbers of bacteroids [55, 56], we hypothesized that GA production confers a selective advantage to rhizobia by increasing nodule size and therefore the number of bacteroids released into the soil upon nodule senescence. To confirm the relationship between nodule size and bacteroid numbers, bacteroids were isolated from mature nodules of varying sizes and counted with flow cytometry to determine the total number of bacteroids, and by plating for colony-forming units (CFUs) to determine the number of viable cells. These analyses confirmed a positive correlation between viable bacteroid cells and larger nodules (**Supplemental Figure 17)**, supporting a selective advantage for larger nodules resulting from rhizobial GA production.

DISCUSSION

Because *cyp115* has been lost from the GA operon found in most rhizobia [15, 18], thereby restricting their ability to directly make bioactive GA, it might have been expected that the resulting production of GA_9, which is not bioactive, would not affect their symbiotic relationship with legumes. However, knockout of the GA operon clearly indicates a phenotypic change with late-stage nodules, thereby indicating that rhizobial production of GA_9 plays a role in such symbiosis. The co-expression of functional soybean GA3ox in the nodules suggested that cooperative production of bioactive GA_4 by these symbiotic partners is possible, and the corresponding ability for low concentrations of bioactive GA_3 to chemically complement the

nodulation phenotype exhibited by ga^- knock-out strains further suggests that such cooperative biosynthesis may be occurring. Though additional experiments will be necessary to confirm such *in planta* conversion of rhizobial GA_9 into GA_4, including analysis of how soybean GA3ox knockouts affect late-stage nodulation phenotypes and more direct observation of GA_9 conversion into GA_4 within the plant, our data provide circumstantial evidence that GA_9 is being supplied by rhizobia to the plant as a precursor for bioactive GA biosynthesis and subsequent signaling that impacts nodulation.

While knocking-out the GA operon affects both nodule numbers and size, consistent with the usual growth-promoting activity associated with GA it is hypothesized here that the primary effect is on size. Accordingly, the increased number of nodules in plants inoculated with ga^- strains presumably results from the need for plants to compensate for the smaller nodule size in order to meet fixed nitrogen requirements. Importantly, increased nodule size provides a direct advantage to the rhizobia that initiated the nodulation event by enabling a larger number of descendants (**Figure 4**). Although it was previously proposed through study of the *Mesorhizobium loti-Lotus japonicus* symbiosis that rhizobial GA acts through suppression of nodulation [14], an increase in nodule size for *L. japonicus* plants inoculated by the GA^+ strains of *M. loti* also was observed. More critically, the competition assay reported in this previous study demonstrated that co-inoculation of *L. japonicus* with equal amounts of GA^+ and ga^- *M. loti* strains led to greater numbers of the GA^+ strain in the resulting nodules. Because the GA operon is only expressed after nodulation [28], co-inoculated GA^+ and ga^- strains should have an equal probability of forming the initial nodules on the legume host. Thus, the observed enrichment in the GA^+ strain from this competition assay indicates that GA production acts locally to increase nodule size rather than exerting a systemic effect restricting nodule formation, particularly as it is unclear how this latter

effect would differentiate between strains with or without the ability to produce GA. By contrast, local activity of rhizobial GA to increase the size of the individual host nodule would provide a direct advantage to the producing strain (i.e., increased number of descendants), regardless of the strains inhabiting other nodules. However, further experimentation will be necessary to understand the mechanism by which rhizobial GA brings about this change in nodule phenotype, not least due to the relatively late-stage effects on nodulation.

The observed increase in nodule size from rhizobial GA may also provide a selective advantage for the host plants, thereby explaining why they enable such manipulation by their rhizobial symbiont (e.g., by expression of the necessary receptor to permit a response to GA). First, as larger nodules have been shown to have a higher ratio of nitrogen-fixing tissue to overall nodule volume than smaller nodules [57–59], this presumably provides nitrogen more efficiently for the host plant. In addition, given that each nodulation event represents opening of the plant interior to microbial invaders [60], the resulting reduced number of nodules may provide an additional advantage in this respect as well. Nevertheless, given the use of bioactive GA as a virulence factor by certain plant pathogens, where it acts to suppress the defense signaling molecule jasmonic acid [37, 61], enabling the nodule to respond to GA may also represent a vulnerability in the host plant defense response. This trade-off may then underlie the observed scattered distribution of the GA operon in rhizobia [18], as only those that partner with legumes whose nodules are open to such manipulation would acquire a selective advantage from such biosynthetic capacity.

If cooperative production of bioactive GA by rhizobia and their host plant is indeed occurring, this phenomenon also must have been driven by the legumes. In particular, it would be beneficial for the host plant to control production of bioactive GA, and thus limit nodule size to

provide only the necessary amount of nitrogen, as well as to attenuate GA production if a microbial defense response, which can be inhibited by GA [61], becomes necessary. This control over GA signaling would presumably underlie the host plant expression of GA3ox genes in nodules, which would remove selective pressure for maintenance of the functionally analogous bacterial *cyp115*, which is almost invariably lost from the GA operon in rhizobia [15, 18]. However, because *cyp115* is maintained as a separate genetic locus undergoing independent horizontal gene transfer within some GA-operon containing rhizobia [15, 18], host plant expression of GA3ox in late stage nodules is presumably not universal, even among those legumes that enable GA signaling in these organs.

Collectively, the results reported here suggest intricate coevolution between GA-producing rhizobia and their legume hosts that may provide selective advantages for both symbionts. Beyond enabling increased nodule growth in response to rhizobial GA, with obvious implications for population growth of GA-producing rhizobia, our data hint at the possibility that legumes may act cooperatively with rhizobia to produce bioactive GA, potentially to balance optimization of nitrogen supply with the microbial defense response.

ACKNOWLEDGEMENTS

This work was supported by grants to R.J.P. from the Iowa Soybean Association and NIH (GM131885).

COMPETING INTERESTS

583 The authors declare no conflict of interest.

584

585 **AUTHOR CONTRIBUTIONS**

586 R.S.N. carried out experimental work and wrote the paper, K.S.B. carried out experimental
587 work, R.J.P. conceived and directed the described work, and helped write the paper.

588

589 **REFERENCES**

590 1. Canfield DE, Glazer AN, Falkowski PG. The evolution and future of Earth's nitrogen
591 cycle. *Science* 2010; **330**: 192–196.

592 2. Ferguson BJ, Indrasumunar A. Soybean Nodulation and Nitrogen Fixation. In: Hendricks
593 BP (ed). *Agricultural Research Updates*, Volume 1. 2011. Nova Science Publishers, Inc.,
594 pp 1–16.

595 3. Udvardi M, Poole PS. Transport and metabolism in legume-rhizobia symbioses. *Annu Rev*
596 *Plant Biol* 2013; **64**: 781–805.

597 4. Oldroyd GED, Murray JD, Poole PS, Downie JA. The rules of engagement in the legume-
598 rhizobial symbiosis. *Annu Rev Genet* 2011; **45**: 119–144.

599 5. Sachs JL, Quides KW, Wendlandt CE. Legumes versus rhizobia: a model for ongoing
600 conflict in symbiosis. *New Phytol* 2018; **219**: 1199–1206.

601 6. Oono R, Denison RF, Kiers ET. Controlling the reproductive fate of rhizobia: How
602 universal are legume sanctions? *New Phytol* 2009; **183**: 967–979.

603 7. Oono R, Denison RF. Comparing symbiotic efficiency between swollen versus
604 nonswollen rhizobial bacteroids. *Plant Physiol* 2010; **154**: 1541–1548.

605 8. Kereszt A, Mergaert P, Kondorosi E. Bacteroid development in legume nodules:
606 Evolution of mutual benefit or of sacrificial victims? *Mol Plant-Microbe Interact* 2011;
607 **24**: 1300–1309.

608 9. Eichmann R, Richards L, Schäfer P. Hormones as go-betweens in plant microbiome
609 assembly. *Plant J* 2020; 518–541.

610 10. MacMillan J. Occurrence of gibberellins in vascular plants, fungi, and bacteria. *J Plant*
611 *Growth Regul* 2002; **20**: 387–442.

612 11. Morrone D, Chambers J, Lowry L, Kim G, Anterola A, Bender K, et al. Gibberellin
613 biosynthesis in bacteria: Separate *ent*-copalyl diphosphate and *ent*-kaurene synthases in
614 *Bradyrhizobium japonicum*. *FEBS Lett* 2009; **583**: 475–480.

615 12. Méndez C, Baginsky C, Hedden P, Gong F, Carú M, Rojas MC. Gibberellin oxidase
616 activities in *Bradyrhizobium japonicum* bacteroids. *Phytochemistry* 2014; **98**: 101–109.

617 13. Nett RS, Montanares M, Marcassa A, Lu X, Nagel R, Charles TC, et al. Elucidation of
618 gibberellin biosynthesis in bacteria reveals convergent evolution. *Nat Chem Biol* 2017; **13**:
619 69–74.

620 14. Tatsukami Y, Ueda M. Rhizobial gibberellin negatively regulates host nodule number. *Sci*
621 *Rep* 2016; **6**: 27998.

622 15. Nett RS, Contreras T, Peters RJ. Characterization of CYP115 as a gibberellin 3-oxidase
623 indicates that certain rhizobia can produce bioactive gibberellin A_4. *ACS Chem Biol* 2017;

12: 912–917.

16. Keister DL, Tully RE, Berkum P Van. A cytochrome P450 gene cluster in the Rhizobiaceae. *J Gen Appl Microbiol* 1999; **45**: 301–303.

17. Hershey DM, Lu X, Zi J, Peters RJ. Functional conservation of the capacity for *ent*-kaurene biosynthesis and an associated operon in certain rhizobia. *J Bacteriol* 2014; **196**: 100–106.

18. Nett RS, Nguyen H, Nagel R, Marcassa A, Charles TC, Friedberg I, et al. Unraveling a tangled skein: Evolutionary analysis of the bacterial gibberellin biosynthetic operon. *mSphere* 2020; **5**: 1–15.

19. Pessi G, Ahrens CH, Rehrauer H, Lindemann A, Hauser F, Fischer H-M, et al. Genome-wide transcript analysis of *Bradyrhizobium japonicum* bacteroids in soybean root nodules. *Mol Plant Microbe Interact* 2007; **20**: 1353–1363.

20. Chang W-S, Franck WL, Cytryn E, Jeong S, Joshi T, Emerich DW, et al. An oligonucleotide microarray resource for transcriptional profiling of *Bradyrhizobium japonicum*. *Mol Plant Microbe Interact* 2007; **20**: 1298–1307.

21. Hauser F, Pessi G, Friberg M, Weber C, Rusca N, Lindemann A, et al. Dissection of the *Bradyrhizobium japonicum* NifA+σ^{54} regulon, and identification of a ferredoxin gene (*fdxN*) for symbiotic nitrogen fixation. *Mol Genet Genomics* 2007; **278**: 255–271.

22. Perret X, Freiberg C, Rosenthal A, Broughton WJ, Fellay R. High-resolution transcriptional analysis of the symbiotic plasmid of *Rhizobium* sp. NGR234. *Mol Microbiol* 1999; **32**: 415–25.

645 23. Li Y, Tian CF, Chen WF, Wang L, Sui XH, Chen WX. High-resolution transcriptomic
646 analyses of *Sinorhizobium* sp. NGR234 bacteroids in determinate nodules of *Vigna*
647 *unguiculata* and indeterminate nodules of *Leucaena leucocephala*. *PLoS One* 2013; **8**:
648 e70531.

649 24. Salazar E, Javier Díaz-Mejía J, Moreno-Hagelsieb G, Martínez-Batallar G, Mora Y, Mora
650 J, et al. Characterization of the NifA-RpoN regulon in *Rhizobium etli* in free life and in
651 symbiosis with *Phaseolus vulgaris*. *Appl Environ Microbiol* 2010; **76**: 4510–4520.

652 25. Sullivan JT, Brown SD, Ronson CW. The NifA-RpoN regulon of *Mesorhizobium loti*
653 strain R7A and its symbiotic activation by a novel LacI/GalR-family regulator. *PLoS One*
654 2013; **8**: e53762.

655 26. Uchiumi T, Ohwada T, Itakura M, Mitsui H, Nukui N, Dawadi P, et al. Expression islands
656 clustered on the symbiosis island of the *Mesorhizobium loti* genome. *J Bacteriol* 2004;
657 **186**: 2439–2448.

658 27. Sarma AD, Emerich DW. Global protein expression pattern of *Bradyrhizobium japonicum*
659 bacteroids: A prelude to functional proteomics. *Proteomics* 2005; **5**: 4170–4184.

660 28. Tatsukami Y, Nambu M, Morisaka H, Kuroda K, Ueda M. Disclosure of the differences
661 of *Mesorhizobium loti* under the free-living and symbiotic conditions by comparative
662 proteome analysis without bacteroid isolation. *BMC Microbiol* 2013; **13**: 180.

663 29. Martinez-Argudo I, Little R, Shearer N, Johnson P, Dixon R. The NifL-NifA system: A
664 multidomain transcriptional regulatory complex that integrates environmental signals. *J*
665 *Bacteriol* 2004; **186**: 601–610.

30. Hayashi S, Gresshoff PM, Ferguson BJ. Mechanistic action of gibberellins in legume nodulation. *J Integr Plant Biol* 2014; **56**: 971–8.

31. Lievens S, Goormachtig S, Den Herder J, Capoen W, Mathis R, Hedden P, et al. Gibberellins are involved in nodulation of *Sesbania rostrata*. *Plant Physiol* 2005; **139**: 1366–79.

32. Ferguson BJ, Ross JJ, Reid JB. Nodulation phenotypes of gibberellin and brassinosteroid mutants of pea. *Plant Physiol* 2005; **138**: 2396–2405.

33. Ferguson BJ, Foo E, Ross JJ, Reid JB. Relationship between gibberellin, ethylene and nodulation in *Pisum sativum*. *New Phytol* 2011; **189**: 829–842.

34. McAdam EL, Reid JB, Foo E. Gibberellins promote nodule organogenesis but inhibit the infection stages of nodulation. *J Exp Bot* 2018; **69**: 2117–2130.

35. Wiemann P, Sieber CMK, von Bargen KW, Studt L, Niehaus EM, Espino JJ, et al. Deciphering the cryptic genome: Genome-wide analyses of the rice pathogen *Fusarium fujikuroi* reveal complex regulation of secondary metabolism and novel metabolites. *PLoS Pathog* 2013; **9**: e1003475.

36. Malonek S, Bömke C, Bornberg-Bauer E, Rojas MC, Hedden P, Hopkins P, et al. Distribution of gibberellin biosynthetic genes and gibberellin production in the Gibberella fujikuroi species complex. *Phytochemistry* 2005; **66**: 1296–1311.

37. Lu X, Hershey DM, Wang L, Bogdanove AJ, Peters RJ. An *ent*-kaurene-derived diterpenoid virulence factor from *Xanthomonas oryzae* pv. *oryzicola*. *New Phytol* 2015; **206**: 295–302.

687 38. Nishijima T, Koshioka M, Yamazaki H. Use of several gibberellin biosynthesis inhibitors
688 in sensitized rice seedling bioassays. *Biosci Biotechnol Biochem* 1994; **58**: 572–573.

689 39. Ueguchi-Tanaka M, Ashikari M, Nakajima M, Itoh H, Katoh E, Kobayashi M, et al.
690 *GIBBERELLIN INSENSITIVE DWARF1* encodes a soluble receptor for gibberellin.
691 *Nature* 2005; **437**: 693–698.

692 40. Nakajima M, Shimada A, Takashi Y, Kim YC, Park SH, Ueguchi-Tanaka M, et al.
693 Identification and characterization of Arabidopsis gibberellin receptors. *Plant J* 2006; **46**:
694 880–889.

695 41. Tully RE, Keister DL. Cloning and mutagenesis of a cytochrome P-450 locus from
696 *Bradyrhizobium japonicum* that is expressed anaerobically and symbiotically. *Appl*
697 *Environ Microbiol* 1993; **59**: 4136–4142.

698 42. Prentki P, Krisch HM. In vitro insertional mutagenesis with a selectable DNA fragment.
699 *Gene* 1984; **29**: 303–313.

700 43. Lenz O, Schwartz E, Dernedde J. The *Alcaligenes eutrophus* H16 *hoxX* gene participates
701 in hydrogenase regulation. *J Bacteriol* 1994; **176**: 4385–4393.

702 44. Cole M a., Elkan GH. Transmissible resistance to penicillin G, neomycin, and
703 chloramphenicol in Rhizobium japonicum. *Antimicrob Agents Chemother* 1973; **4**: 248–
704 253.

705 45. Fu C, Maier RJ. Identification of a locus within the hydrogenase gene cluster involved in
706 intracellular nickel metabolism in *Bradyrhizobium japonicum*. *Appl Environ Microbiol*
707 1991; **57**: 3502–3510.

46. Maekawa T, Maekawa-Yoshikawa M, Takeda N, Imaizumi-Anraku H, Murooka Y, Hayashi M. Gibberellin controls the nodulation signaling pathway in *Lotus japonicus*. *Plant J* 2009; **58**: 183–194.

47. Han F, Zhu B. Evolutionary analysis of three gibberellin oxidase genes in rice, Arabidopsis, and soybean. *Gene* 2011; **473**: 23–35.

48. Binks R, MacMillan J, Pryce RJ. Combined gas chromatography-mass spectrometry of the methyl esters of gibberellins A_1 to A_{24} and their trimethylsilyl ethers. *Phytochemistry* 1969; **8**: 271–84.

49. Lee HI, Lee JH, Park KH, Sangurdekar D, Chang WS. Effect of soybean coumestrol on *Bradyrhizobium japonicum* nodulation ability, biofilm formation, and transcriptional profile. *Appl Environ Microbiol* 2012; **78**: 2896–2903.

50. Libault M, Thibivilliers S, Bilgin DD, Radwan O, Benitez M, Clough SJ, et al. Identification of four soybean reference genes for gene expression normalization. *Plant Genome J* 2008; **1**: 44.

51. Ritchie, S.W., Hanway, J.J., Thompson HE. How a soybean plant develops. Spec. Rep. No. 53. 1994. Ames, IA.

52. Severin AJ, Woody JL, Bolon Y-T, Joseph B, Diers BW, Farmer AD, et al. RNA-Seq Atlas of Glycine max: a guide to the soybean transcriptome. *BMC Plant Biol* 2010; **10**: 160.

53. Libault M, Farmer A, Joshi T, Takahashi K, Langley RJ, Franklin LD, et al. An integrated transcriptome atlas of the crop model Glycine max, and its use in comparative analyses in

plants. *Plant J* 2010; **63**: 86–99.

54. Fleet CM, Sun TP. A DELLAcate balance: The role of gibberellin in plant morphogenesis. *Curr Opin Plant Biol* 2005; **8**: 77–85.

55. Kiers ET, Rousseau R a, West S a, Denison RF. Host sanctions and the legume-rhizobium mutualism. *Nature* 2003; **425**: 78–81.

56. Simms EL, Taylor DL, Povich J, Shefferson RP, Sachs JL, Urbina M, et al. An empirical test of partner choice mechanisms in a wild legume-rhizobium interaction. *Proc Biol Sci* 2006; **273**: 77–81.

57. Chen HK, Thornton HG. The structure of 'ineffective' nodules and its influence on nitrogen fixation. *Proc R Soc London B* 1940; **129**: 208–229.

58. Aprison MH, Magee WE, Burris RH. Nitrogen fixation by excised soy bean root nodules. *J Biol Chem* 1954; **208**: 29–39.

59. Tajima R, Lee ON, Abe J, Lux A, Morita S. Nitrogen-fixing activity of root nodules in relation to their size in peanut (Arachis hypogaea L.). *Plant Prod Sci* 2007; **10**: 423–429.

60. Berrabah F, Ratet P, Gourion B. Legume nodules: Massive infection in the absence of defense induction. *Mol Plant-Microbe Interact* 2019; **32**: 35–44.

61. Navarro L, Bari R, Achard P, Lisón P, Nemri A, Harberd NP, et al. DELLAs control plant immune responses by modulating the balance of jasmonic acid and salicylic acid signaling. *Curr Biol* 2008; **18**: 650–655.

FIGURE LEGENDS

Figure 1. GA biosynthetic operon in *B. diazoefficiens* USDA 110. The product of the GA operon (*blr2143-blr2150*) is non-bioactive GA_9. However, a single hydroxylation of this compound produces GA_4, a bioactive phytohormone.

Figure 2. Effect of GA operon knockout in the *Bradyrhizobium*-soybean symbiosis. Soybean plants were nodulated with either wild-type, GA-producing *B. diazoefficiens* USDA 110 (GA^+) or the GA operon-knockout *B. diazoefficiens* KB2011 (ga^-). Representative plants (n = 6) were harvested at four time points (vegetative, flowering, early pod, and full pod stages) to measure the following phenotypes: **A**) Average plant height, **B**) plant fresh mass, **C**) the average number of nodules per plant, **D**) the average mass per nodule for each plant, and **E**) average total nodule mass per plant. **F)** Nodule size distribution of soybean nodulated with GA^+ or ga^- *B. diazoefficiens*. The diameters of individual nodules collected at the soybean full pod stage were measured and binned into defined size groups. The distribution of nodule sizes are represented as the percentage of the total nodule number of the plant. n = 6 plants per condition at each time point. For all bar graphs, the mean is shown with ± standard deviation (SD). Statistical significance was assessed at each time point using an unpaired, two-tailed t-test; n.s. = not significant ($p > 0.05$). Individual p values are shown when ≤ 0.1.

Figure 3. Chemical complementation with GA_3 restores nodulation phenotypes to GA knockout. The soil substrate of soybeans nodulated by GA^+ or ga^- *B. diazoefficiens* was treated weekly with 1, 10, or 100 nM GA_3 in water, or GA-free water as a negative control. The following phenotypes were measured at the early pod stage: **a**) number of nodules per plant **b**) average mass per nodule, and **c**) total nodule mass. **d)** Representative root nodules from each experimental group. Each image shows nodules isolated from one plant. n = 7 for each treatment. Shown for each experimental group is the mean ± SD. Statistical significance was assessed using a two-way ANOVA and Dunnett's multiple comparison test with the GA^+ water treatment as the control group. n.s. indicates $p > 0.05$. Individual p values are shown when ≤ 0.1.

Figure 4. Proposed model for the function of rhizobial GA in symbiosis. Produce either non-bioactive GA_9 or bioactive GA_4 during symbiosis, depending on whether the rhizobial species has *cyp115*. If GA_9 is the final product, we propose that host plant GA 3-oxidases convert GA_9 into bioactive GA_4. GA signaling then leads to an increase in nodule size, which increases bacteroid numbers within that nodule and more rhizobia released into the soil upon nodule senescence. Conversely, an absence of rhizobial GA results in decreased nodule size and thus fewer bacteria being released per nodule.

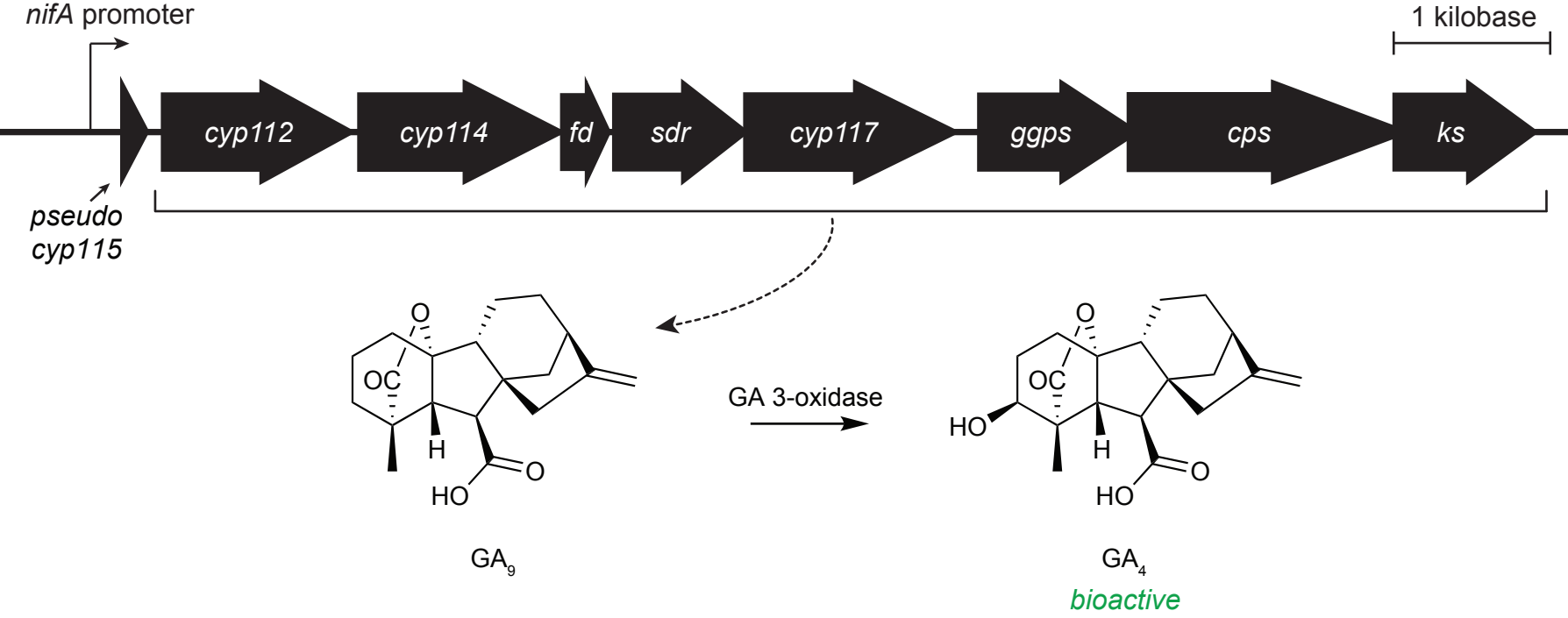
nifA promoter
1 kilobase
cyp112
cyp114
fd
sdr
cyp117
ggps
cps
ks
pseudo cyp115
GA 3-oxidase
GA9
GA4
bioactive

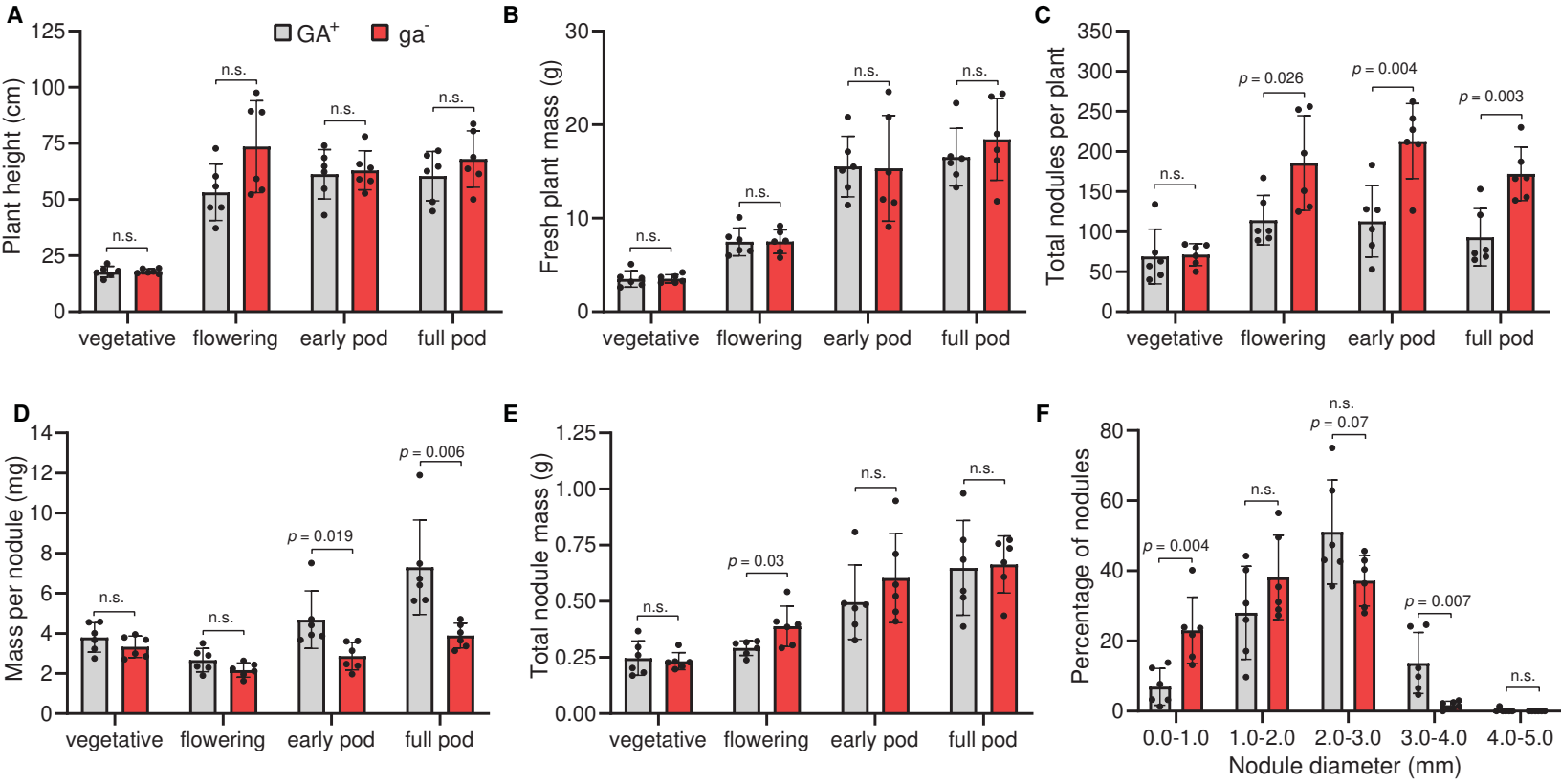
A
GA+
ga-
Plant height (cm)
125
100
75
50
25
0
n.s.
n.s.
n.s.
n.s.
vegetative
flowering
early pod
full pod
B
Fresh plant mass (g)
30
20
10
0
n.s.
n.s.
n.s.
n.s.
vegetative
flowering
early pod
full pod
C
Total nodules per plant
350
300
250
200
150
100
50
0
n.s.
p = 0.026
p = 0.004
p = 0.003
vegetative
flowering
early pod
full pod
D
Mass per nodule (mg)
14
12
10
8
6
4
2
0
n.s.
n.s.
p = 0.019
p = 0.006
vegetative
flowering
early pod
full pod
E
Total nodule mass (g)
1.25
1.00
0.75
0.50
0.25
0.00
n.s.
p = 0.03
n.s.
n.s.
vegetative
flowering
early pod
full pod
F
Percentage of nodules
80
60
40
20
0
p = 0.004
n.s.
n.s.
p = 0.07
p = 0.007
n.s.
0.0-1.0
1.0-2.0
2.0-3.0
3.0-4.0
4.0-5.0
Nodule diameter (mm)

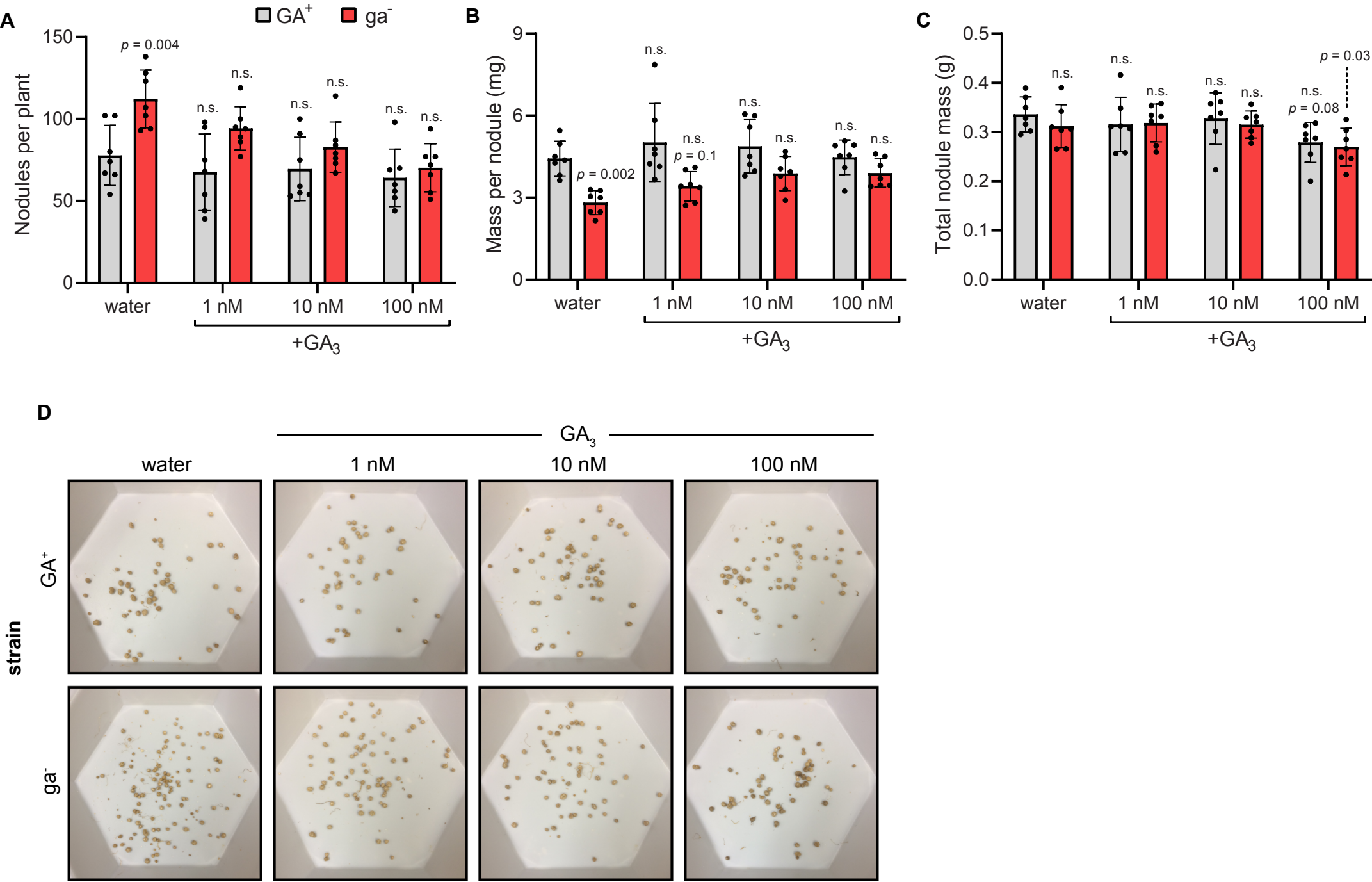
A
GA+
ga-
Nodules per plant
150
100
50
0
p = 0.004
n.s.
water
1 nM
10 nM
100 nM
+GA3
B
Mass per nodule (mg)
9
6
3
0
p = 0.002
p = 0.1
C
Total nodule mass (g)
0.5
0.4
0.3
0.2
0.1
0.0
p = 0.08
p = 0.03
D
GA3
strain
GA+
ga-

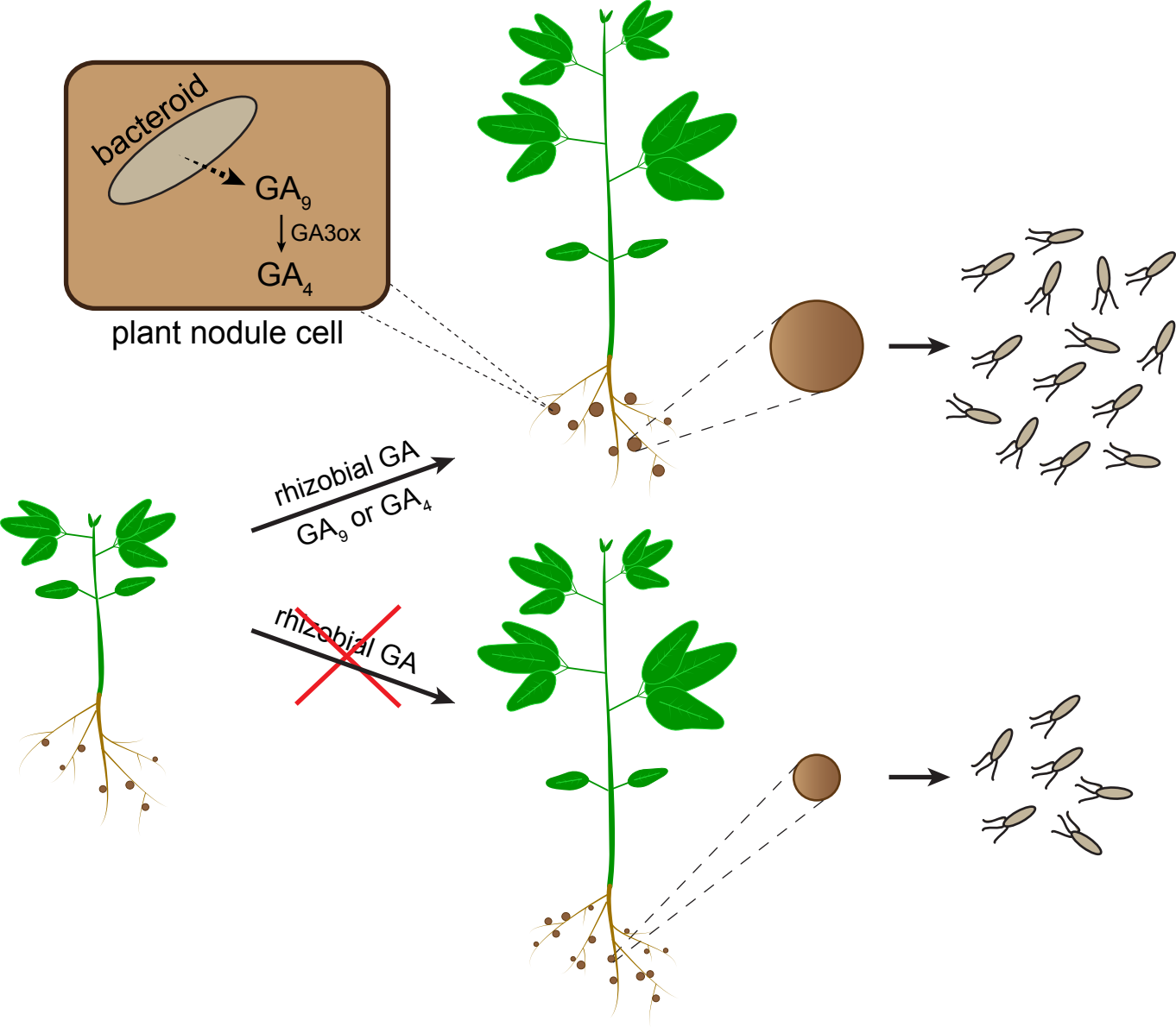
bacteroid
GA9
GA3ox
GA4
plant nodule cell
rhizobial GA
GA9 or GA4
rhizobial GA

SUPPLEMENTARY INFORMATION

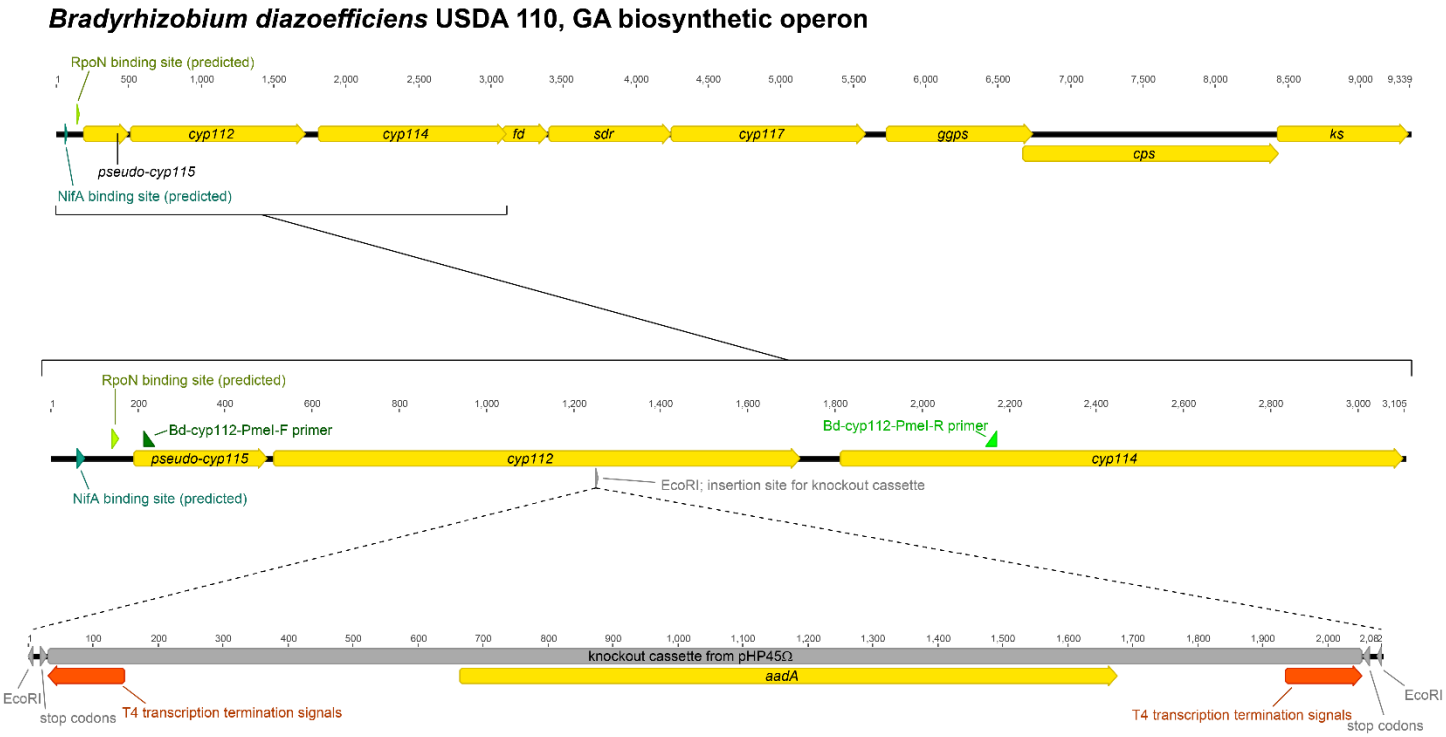

Supplementary Figure 1. Schematic of GA operon knockout strategy. Polar knockouts of the GA operon in *Bradyrhizobium diazoefficiens* USDA 110 were constructed by inserting a knockout cassette containing *aadA* and flanking terminators (derived from pHP45Ω [1]) into *cyp112*.

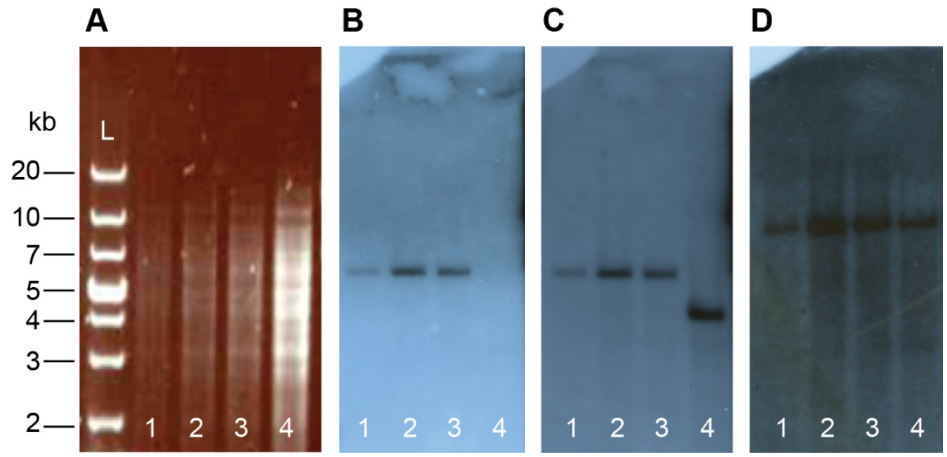

Supplementary Figure 2. Southern blot analysis of *B. diazoefficiens* USDA 110 GA operon knockout strains KB0903, KB0904, and KB2011. **A**) Agarose gel of XhoI gDNA digests. The gel was loaded as follows: L = DNA ladder, 1 = KB0903, 2 = KB0904, 3 = KB2011, and 4 = *B. diazoefficiens* USDA 110 (wild type). Panels **B-D** are blots of the gel in panel **A** probed with the following: **B**) *aadA*, **C**) *cyp112*, **D**) *cyp114.* kb = kilobase

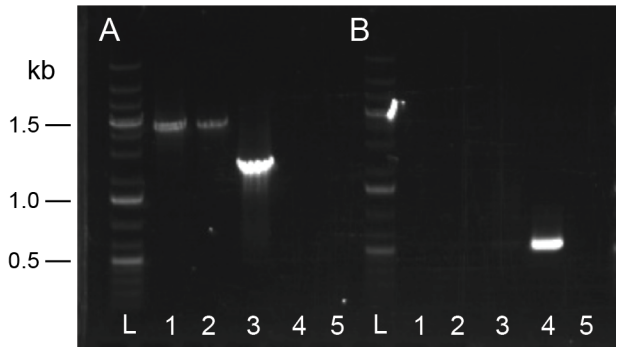

Supplementary Figure 3. **PCR analysis of *B. diazoefficiens* USDA 110 GA operon knockout strains KB0904 and KB2011. a**) PCR with primer set targeting the chromosomal region outside of the insertion of the *aadA* interruption cassette (primers bind to the *pseudo cyp115* and *cyp114* genes). **b**) PCR with primer set targeting the *sacB* gene of the pLOBJ3 suicide vector used for introducing the interruption cassette. Lanes 1-5 correspond to the following template DNA: 1 = KB2011, 2 = KB0904, 3 = *B. diazoefficiens* USDA 110 (wild type), 4 = pLOBJ3 mating vector, and 5 = no DNA; L = DNA ladder. kb = kilobase

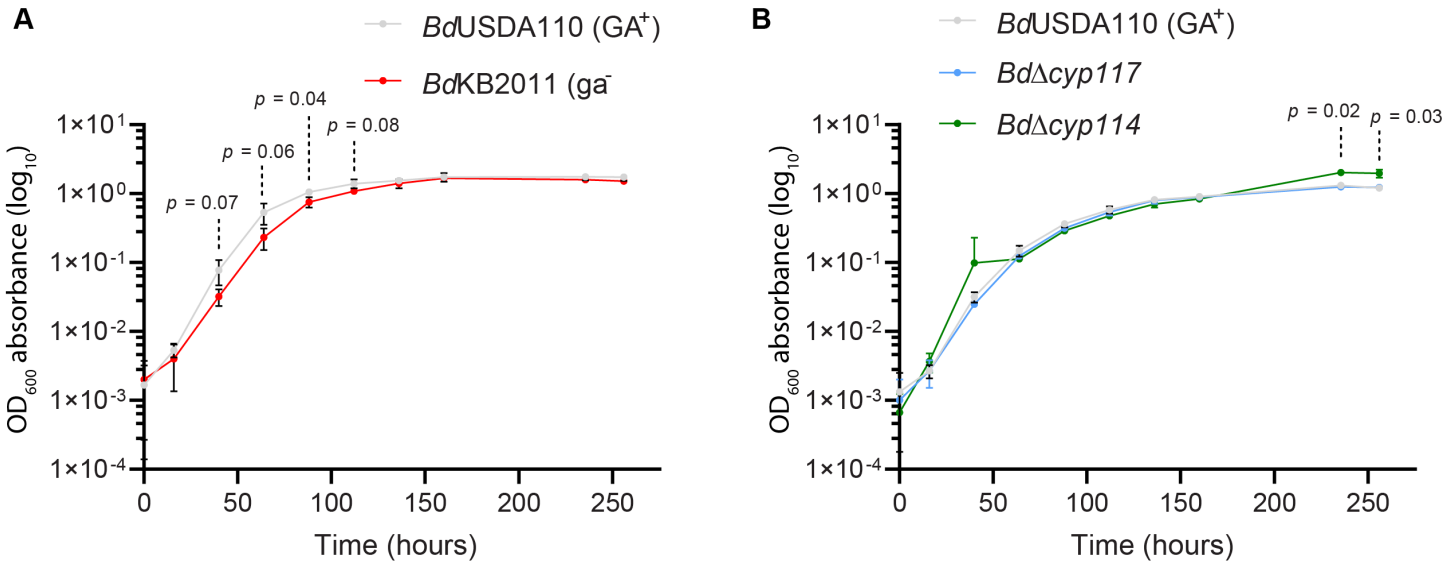

Supplementary Figure 4. Aerobic growth curves of *B. diazoefficiens* USDA110 (GA$^+$) and GA operon mutants. A) GA$^+$ (*Bd*USDA110) growth compared to that of ga$^-$ (*Bd*KB2011), as measured by the optical density of the cultures measured at a wavelength of 600 nm (OD_{600}). Note that the y-axis is on a $\log_{10}$ scale. Statistical significance for each time point was determined with an unpaired t-test. *P*-values less than 0.1 are shown above the relevant time points. All other time points had a *P*-value > 0.1. n = 3 cultures for each strain with the mean ± SD shown. **B)** GA$^+$ growth compared to that of *cyp117* and *cyp114* deletion mutants (*BdΔcyp117* and *BdΔcyp114*, respectively). Note that the y-axis is on a $\log_{10}$ scale. n = 3 cultures for each strain with the mean ± SD shown. After 40 hours, one of the GA$^+$ cultures was contaminated, so only two replicates were measured for subsequent time points. Statistical significance for each time point was determined with separate unpaired t-tests between GA$^+$/*BdΔcyp117* and GA$^+$/*BdΔcyp114*. All *p* values were > 0.05 except for those indicated in the figure for *BdΔcyp114*.

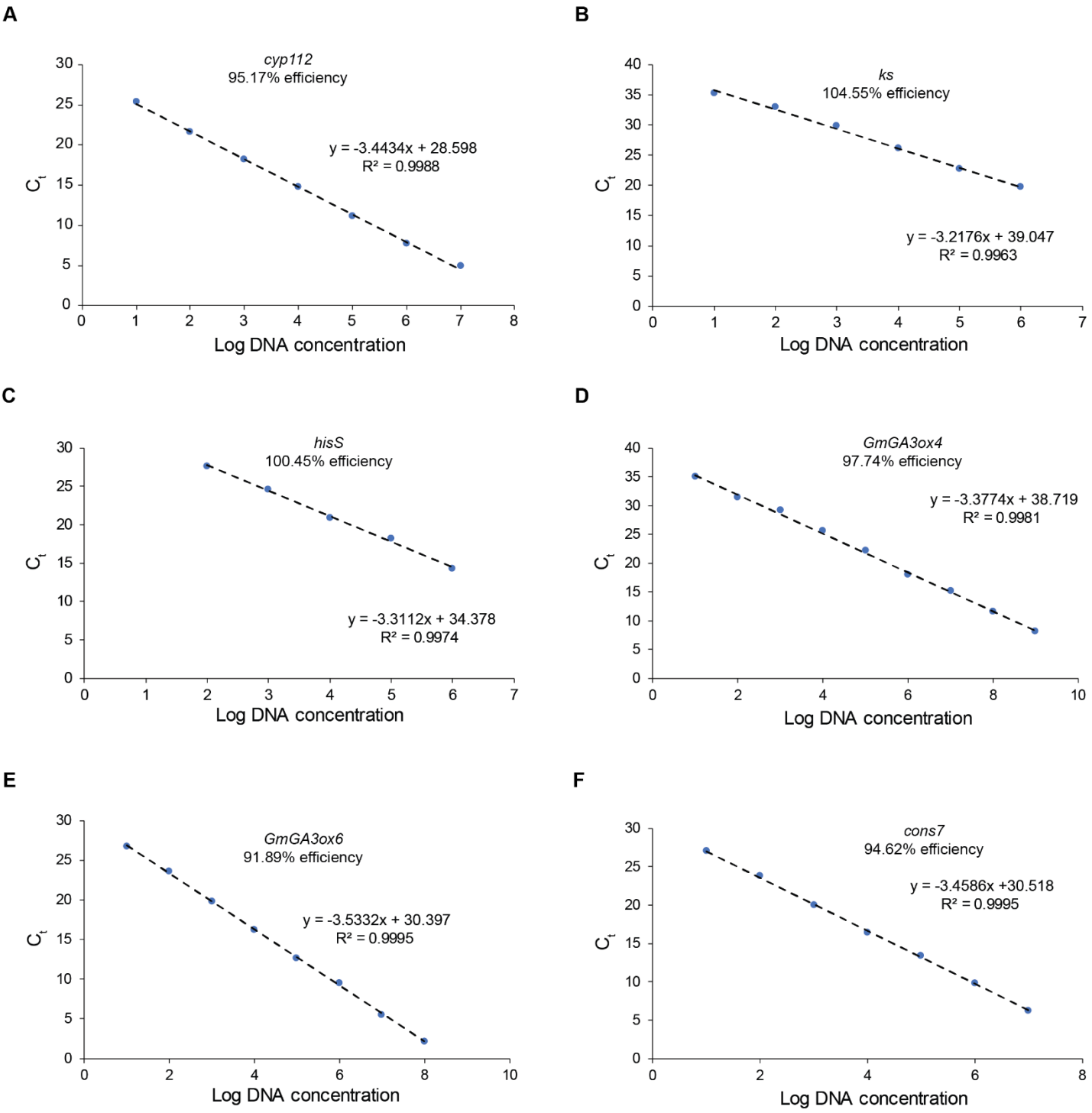

Supplementary Figure 5. qPCR primer efficiencies. Shown are the calculated cycle threshold (C_t) values plotted against the corresponding DNA template concentration (log scale) for the qPCR primer sets used to quantify expression for **A**) *cyp112*, **B**) *ks*, and **C**) *hisS* (reference gene) from *B. diazoefficiens* USDA 110, along with **D**) *GA3ox4*, **E**) *GA3ox6*, and **F**) *cons7* (reference gene) from *G. max* cv. Williams ’82.

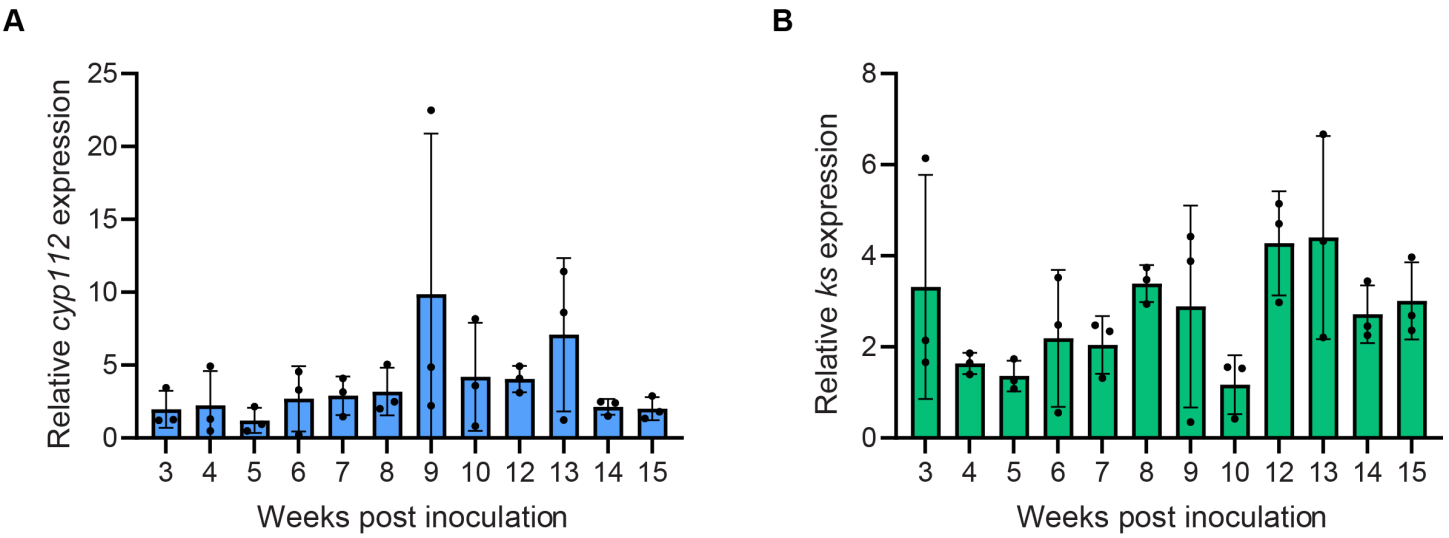

Supplementary Figure 6. Expression of GA operon genes during the *Bradyrhizobium diazoefficiens*-soybean symbiosis. Bacteroid expression of **A**) *cyp112* and **B**) *ks* over the course of *B. diazoefficiens* USDA 110 symbiosis with soybean. Target gene expression was normalized using *B. diazoefficiens* USDA 110 *hisS* as a reference gene, and relative expression was then calculated by dividing all values by the lowest mean expression value of the data set. n = 3 biological replicates (nodules derived from three different plants) for each time point with ± standard deviation (SD) shown.

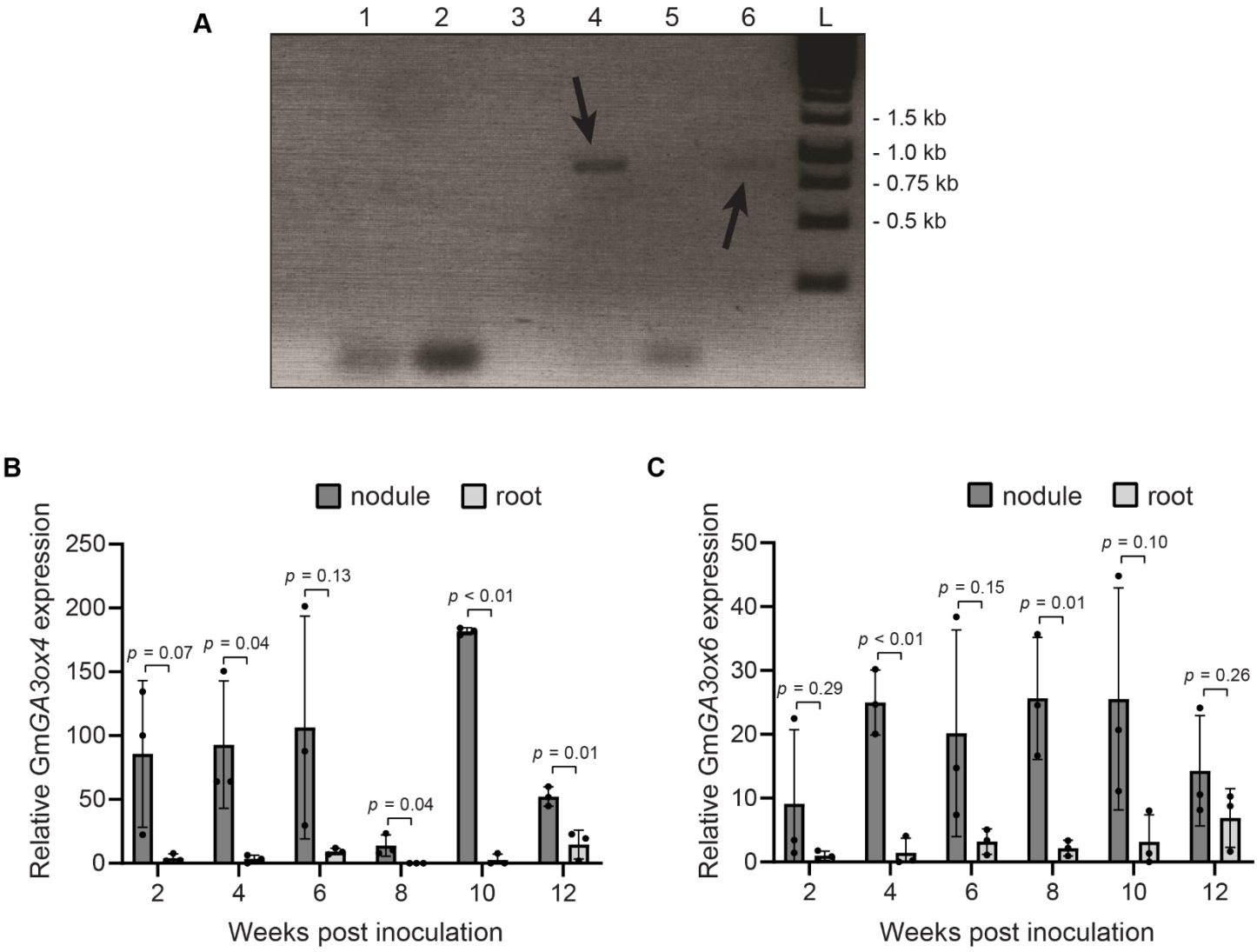

Supplementary Figure 7. Expression of soybean GA 3-oxidase isoforms in nodule tissue. A) PCR with cDNA isolated from mature nodules (during flowering stage) demonstrates that two isoforms are noticeably expressed in this tissue, as shown via agarose gel analysis. Primers for this PCR were design to produce amplicons of roughly 800-1000 base pairs. Arrows indicate detected amplicon bands. 1: Gm*GA3ox1*, 2: Gm*GA3ox2*, 3: Gm*GA3ox3*, 4: Gm*GA3ox4*, 5: Gm*GA3ox5*, 6: Gm*GA3ox6*, L: DNA ladder. kb = kilobase. Expression of **B)** Gm*GA3ox4* and **C)** Gm*GA3ox6* was confirmed via qPCR analysis of cDNA prepared from soybean nodule and root tissue over 12 weeks of development. Target gene expression was normalized using *G. max* cv. Williams '82 *cons7* as a reference gene, and relative expression was then calculated by dividing values by the mean expression value of the lowest mean within the data set. n = 3 for each tissue at each time point. Each replicate represents cDNA samples prepared from tissue derived from different plants. Shown for each condition is the mean ± SD. Statistical comparisons for each time point were made using two-tailed t-tests.

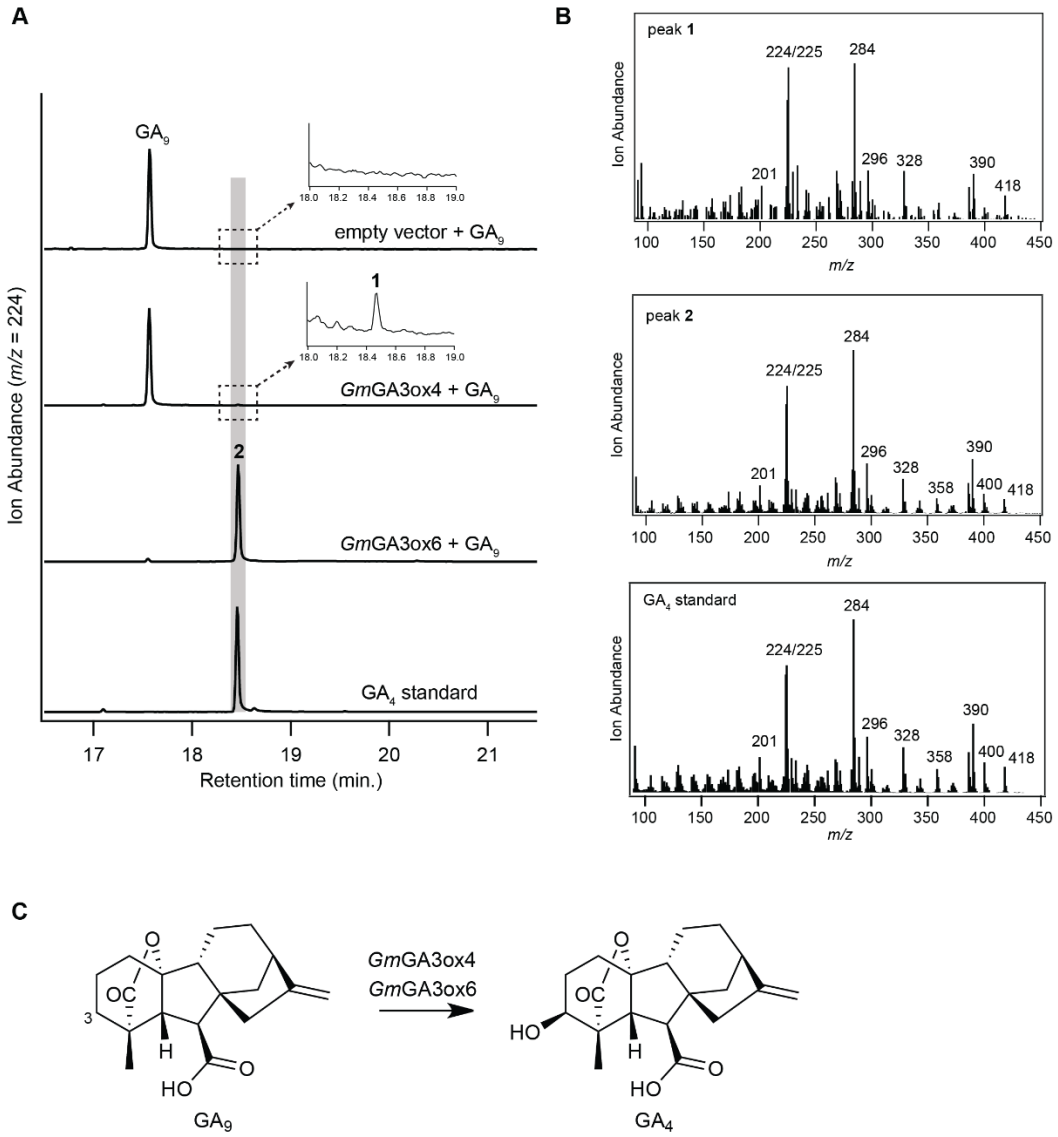

Supplementary Figure 8. Confirmation of GA 3-oxidase activity by *Gm*GA3ox4 and *Gm*GA3ox6. A) Incubating GA_9 in cells expressing synthetic clones of either *Gm*GA3ox4 or *Gm*GA3ox6 results in consumption of GA_9 and production of GA_4, as shown here through extracted ion chromatograms from GC-MS analysis. **B**) Mass spectra of the putative GA_4 products and an authentic GA_4 standard. The chromatograms and spectra shown are representative of the methyl ester (GA_9) or methyl ester, trimethylsilyl ether (GA_4) of the corresponding compounds. **C)** Reaction proposed to be catalyzed by *Gm*GA3ox4 and *Gm*GA3ox6 - 3β-hydroxylation of GA_9 to produce bioactive GA_4.

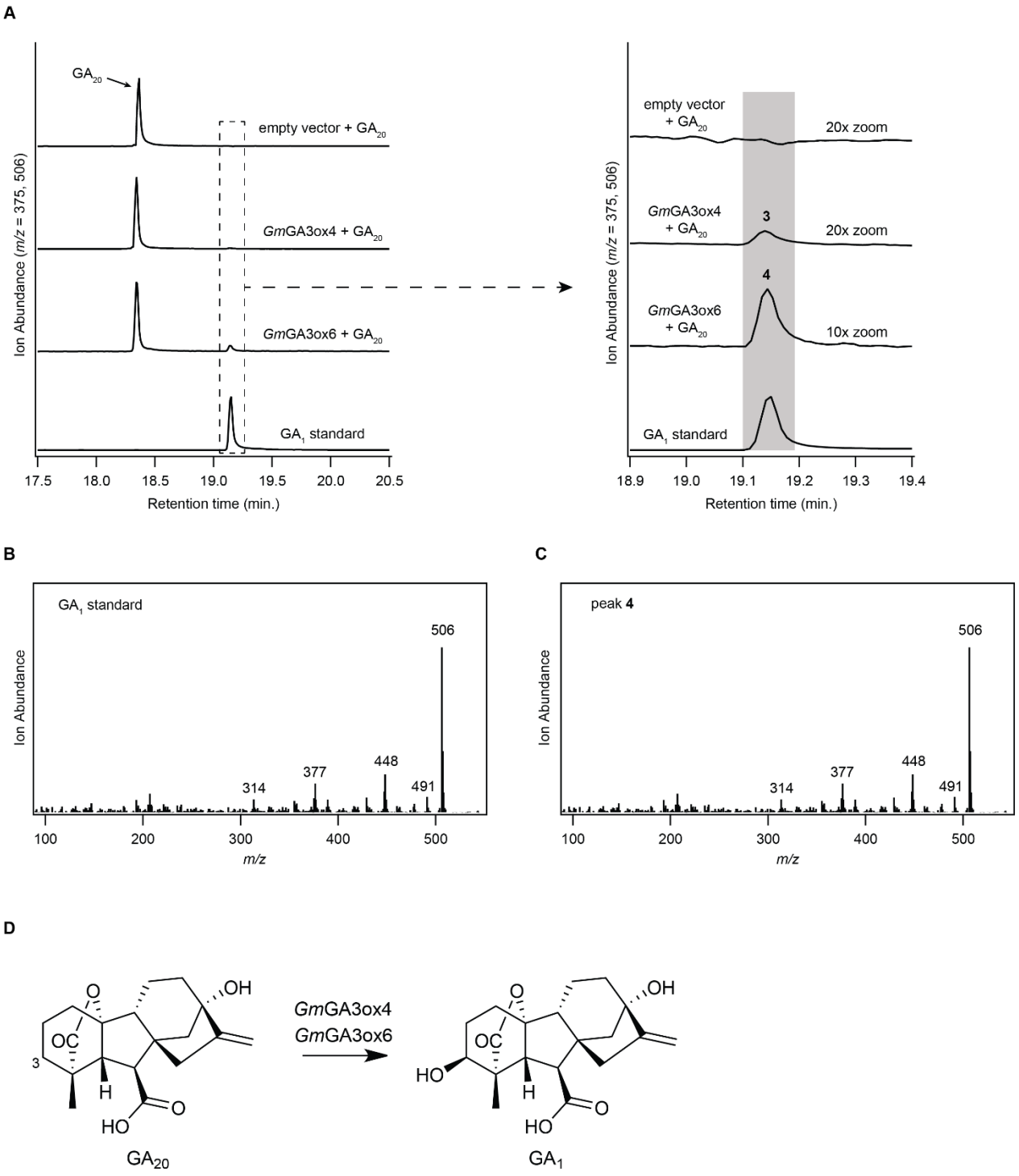

Supplementary Figure 9. *Gm*GA3ox4 and *Gm*GA3ox6 exhibit GA 3-oxidase activity with GA_{20}. A) Incubation of GA_{20} in *E. coli* cells expressing either *Gm*GA3ox4 or *Gm*GA3ox6 results in formation of GA_1, as shown here via extracted ion chromatograms from GC-MS analysis. **B**) Mass spectrum of an authentic GA_1 standard. **C**) Mass spectrum of peak **4**, a putative GA_1 peak produced from incubation of GA_{20} with *Gm*GA3ox6-expressing cells. The abundance of peak **3** was too low for a high-quality mass spectrum to be derived. The chromatograms and spectra shown are representative of the methyl ester, trimethylsilyl ether of the corresponding compounds. **D)** Proposed 3β-hydroxylation of GA_{20} by *Gm*GA3ox4 and *Gs*GA3ox6 to produce bioactive GA_1.

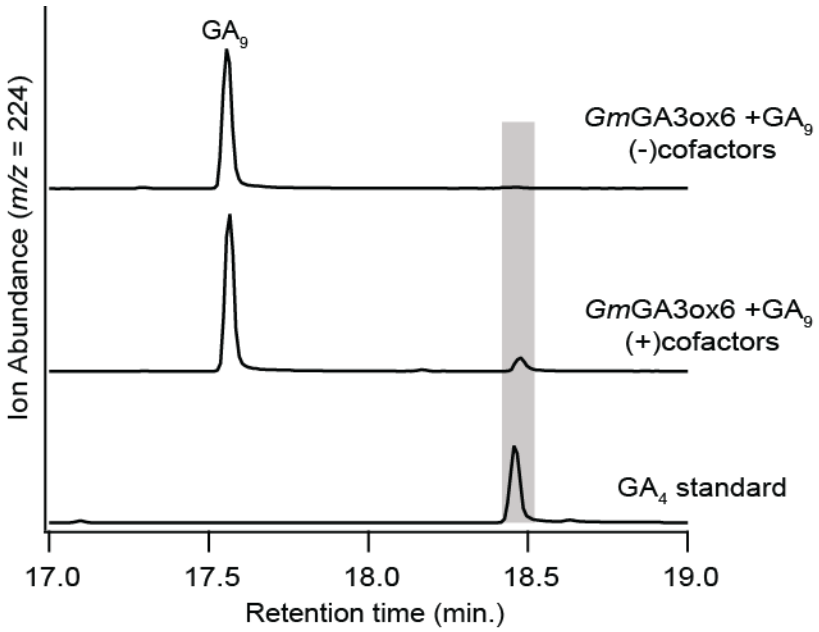

Supplementary Figure 10. Confirmation of *Gm*GA3ox6 as a 2ODD enzyme. Lysates from cells expressing *Gm*GA3ox6 were incubated with GA_9 in either the presence or absence of Fe(II)/2-oxoglutarate dependent dioxygenase (2ODD) cofactors (2-oxoglutarate, ascorbate, and iron). Production of GA_4 was detected with GC-MS, as shown here with representative extracted ion chromatograms. The chromatograms shown correspond to the methyl ester (GA_9) or methyl ester, trimethylsilyl ether (GA_4) of the corresponding compounds. Due to the high homology and similar functionality demonstrated between *Gm*GA3ox4 and *Gm*GA3ox6, the status of *Gm*GA3ox4 as a 2ODD enzyme is inferred.

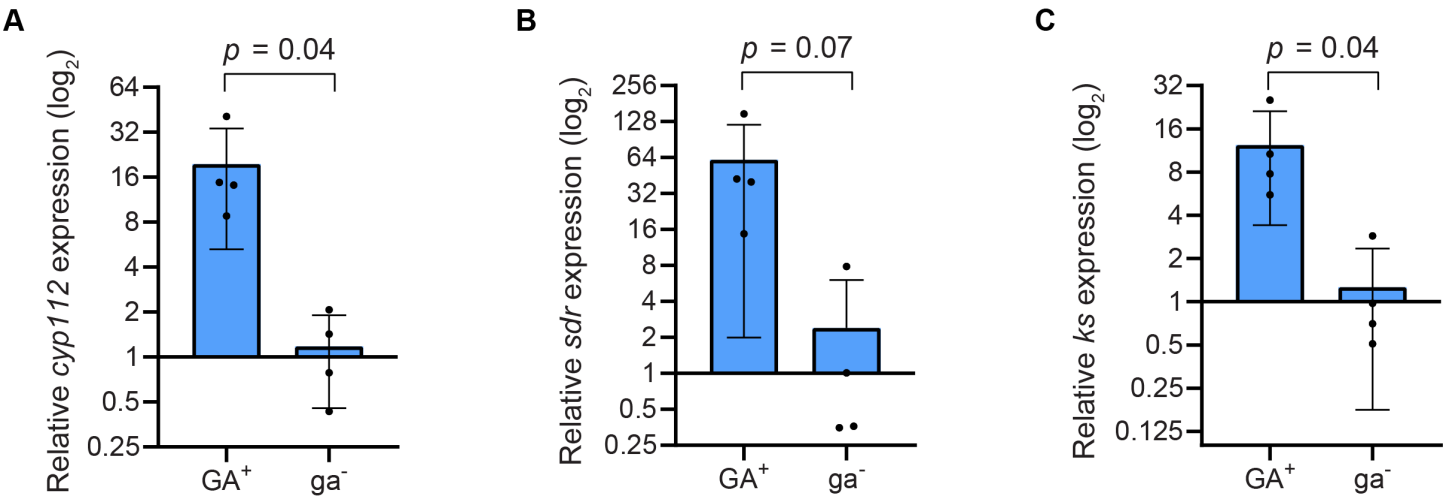

Supplementary Figure 11. Expression of GA operon genes in GA$^+$ and ga$^-$ *B. diazoefficiens* bacteroids. Relative expression of **A**) *cyp112*, **B**) *sdr*, and **C**) *ks* as determined via qPCR with cDNA generated from post-flowering stage GA$^+$ or ga$^-$ bacteroids. Target gene expression was normalized using *B. diazoefficiens* USDA 110 *hisS* as a reference gene, and relative expression was then calculated by dividing values by the mean expression value of the corresponding ga$^-$ expression data. n = 4 biological replicates with ± SD shown. Data is shown on a $\log_2$ scale, with statistics performed on the non-log-transformed data. Statistical significance was assessed using a one-tailed Welch's t-test. Trace amounts of GA operon gene amplification in the ga$^-$ strain are presumably due to low levels of contaminating bacterial gDNA.

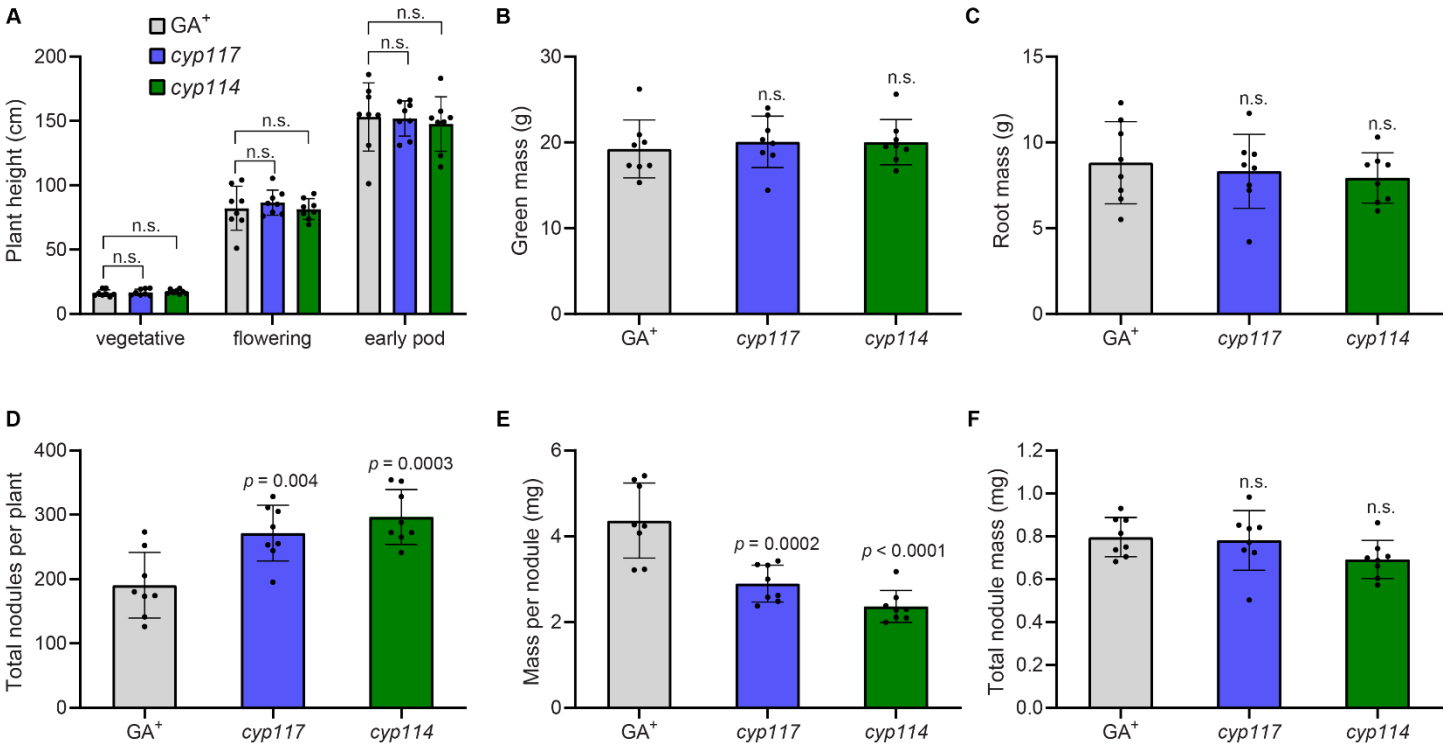

Supplementary Figure 12. Soybean phenotypes associated with knockout of *cyp117* and *cyp114* in *B. diazoefficiens*. Soybean plants were inoculated with wild-type (GA^+) *B. diazoefficiens*, or with strains containing a knockout of *cyp117* (*BdΔcyp117* or *cyp114* (*BdΔcyp114*). **A**) Plant height was measured for three different time points. At the early pod stage of the plants, the following phenotypic parameters were assessed: **B**) green mass, **C**) root mass, **D**) nodule number per plant, **E**) average mass per nodule, and **F**) total nodule mass per plant. n = 8 for each treatment with means ± SD shown. Statistical significance was assessed by using a two-way ANOVA and Dunnett's multiple comparison test with GA^+ as the control group. n.s. = not significant ($p > 0.05$). For height measurements, statistical significance was determined between treatments within a single time point.

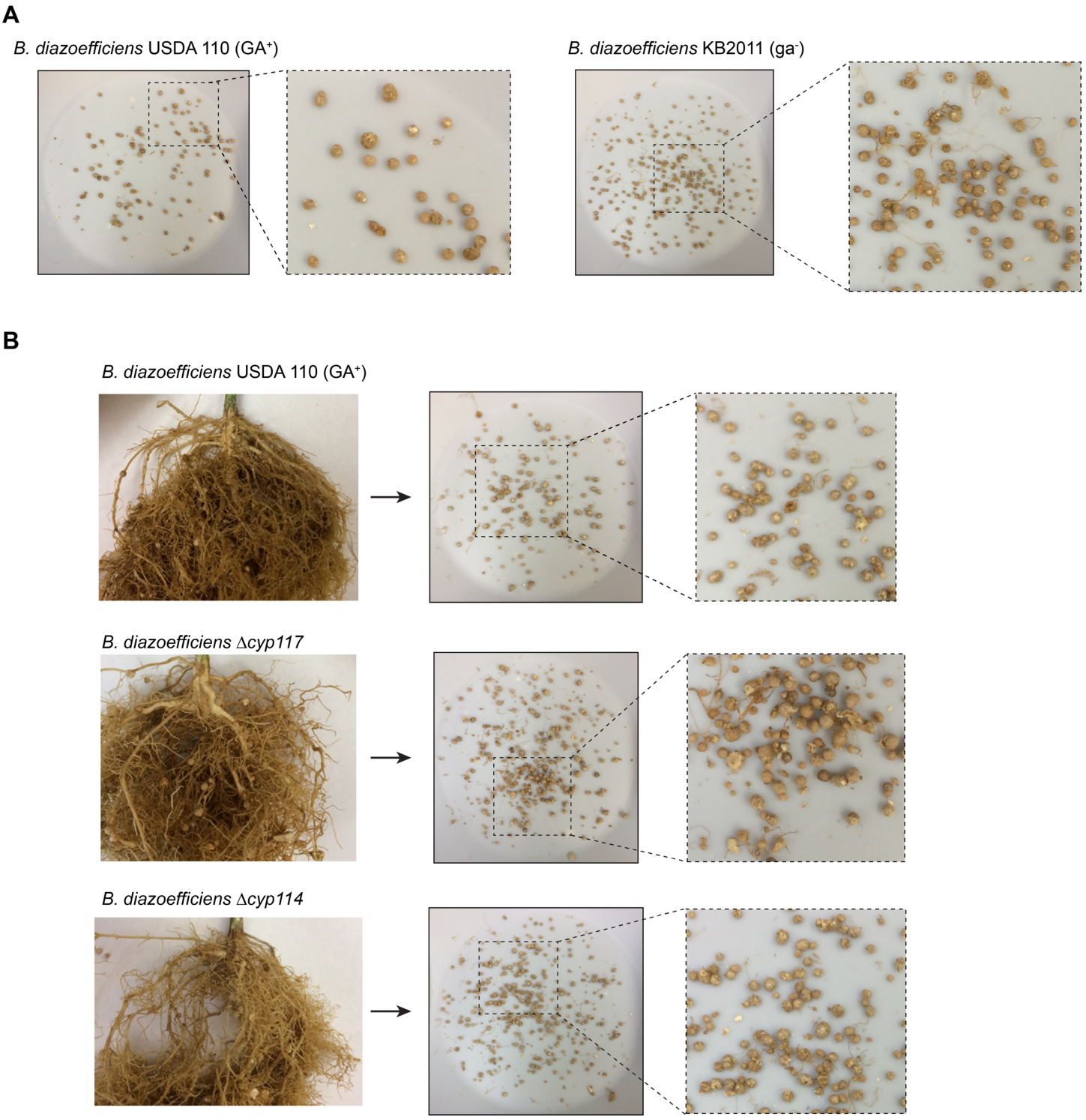

Supplementary Figure 13. Representative images of GA$^+$ and ga$^-$ nodules. A) All of the nodules from single representative *B. diazoefficiens* USDA 110 (GA+) and *B. diazoefficiens* KB2011 (ga-) plants are shown, as well as zoomed in images to better demonstrate nodule morphology and appearance. Each of these plants were from the same experiment. **B)** Roots, total nodules, and zoomed in nodule images from representative GA+, *Bd*Δ*cyp117*, and *Bd*Δ*cyp114* plants. These plants were all from the same experiment.

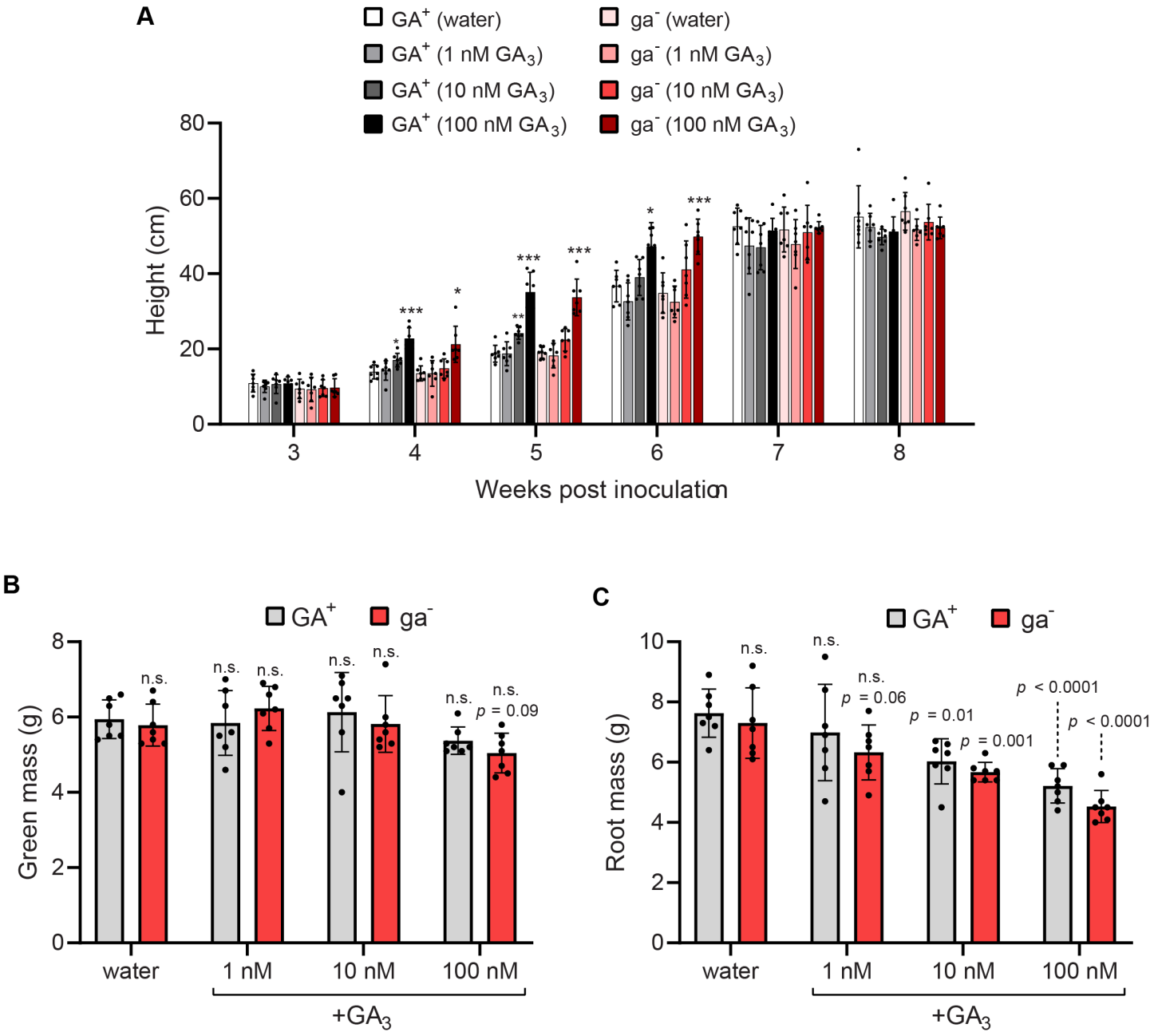

Supplementary Figure 14. Effects of a range of GA_3 concentrations on plant height and mass. The soil substrate of soybean plants in symbiosis with either GA^+ or ga^- *B. diazoefficiens* were treated with several concentrations of GA_3 (1, 10, or 100 nM) or water. **A**) Plant height was measured over time. The following phenotypic measurements were assessed at the early pod stage: **B**) green mass and **C**) root mass. n = 7 for each treatment with means ± SD shown. Statistical significance was assessed using a two-way ANOVA and Dunnett's multiple comparison test, with the GA^+ water treatment used as the control. n.s. = not significant ($p > 0.05$). For height measurements, statistical significance was only assessed between experimental treatments within a single time point. * = $p < 0.05$, ** = $p < 0.01$, *** = $p < 0.001$. An absence of asterisks in panel "a" infers $p > 0.05$. Individual p values are shown if ≤ 0.1.

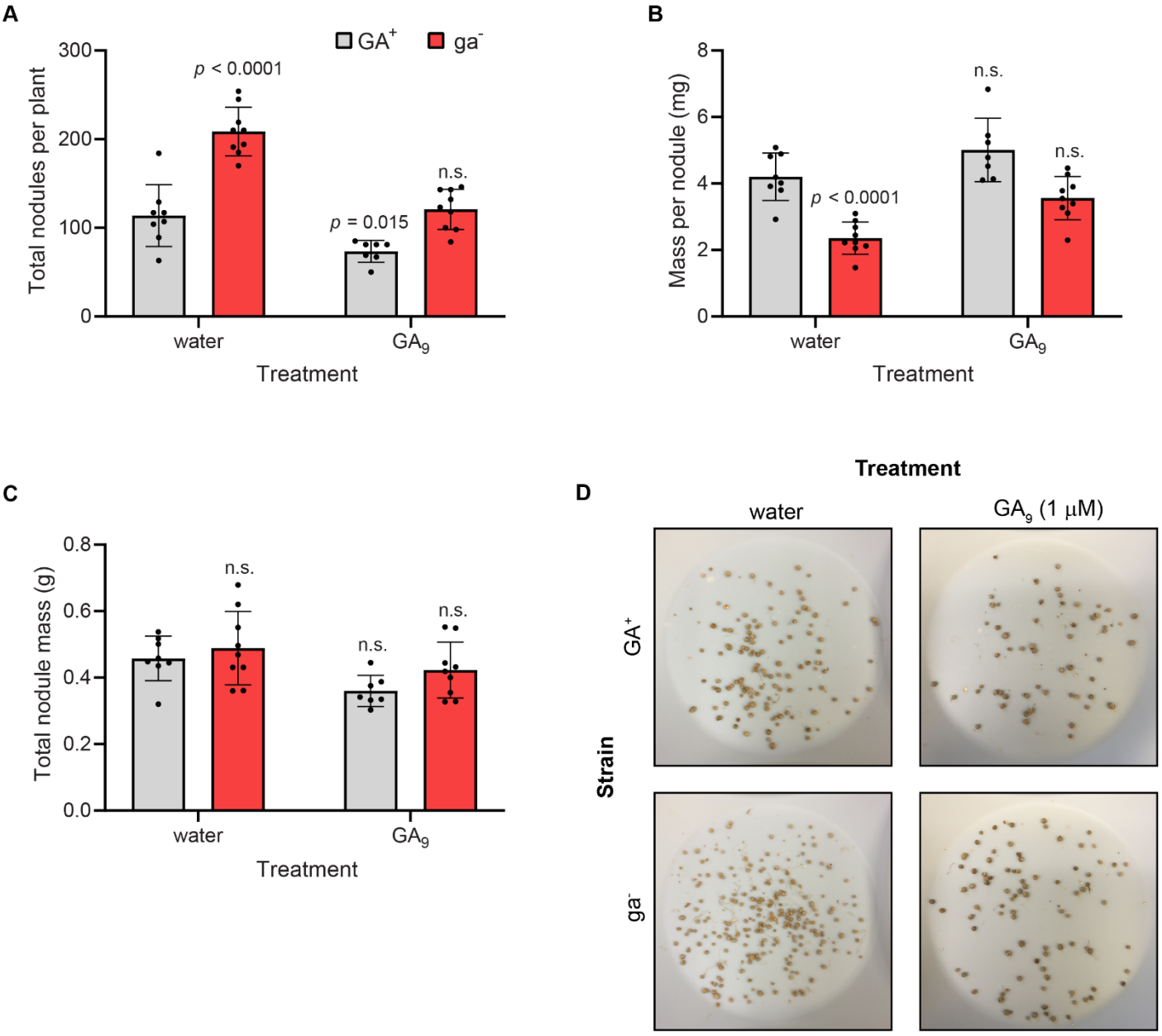

Supplementary Figure 15. Chemical complementation with GA_9 rescues the ga⁻ nodule phenotypes. Nodule phenotypic characteristics were measured at the early pod stage following weekly application of GA_9 (1 µM) to the soil substrate of soybean plants nodulated with GA^+ or ga⁻ *B. diazoefficiens*. **A**) Average number of nodules per plant. **B**) Average mass per nodule. **C**) Total nodule pass per plant. **D)** Representative root nodules from each experimental group. Each image shows nodules isolated from one plant. n = 7-9 plants per treatment. Shown for each experimental group is the mean ± SD. Statistical significance was assessed using a two-way ANOVA and Dunnett's multiple comparison test with the GA^+ water treatment as the control group. n.s. indicates $p > 0.05$. Individual p values are shown when ≤ 0.1.

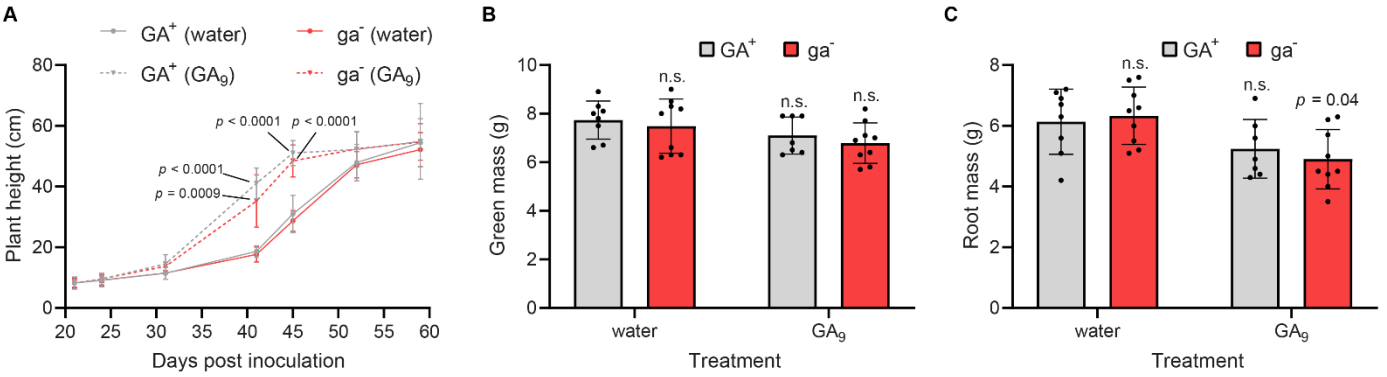

Supplementary Figure 16. Effect of exogenous GA_9 on soybean growth phenotypes. Following nodulation of soybean plants with GA^+ and ga^- *B. diazoefficiens*, 1 µM GA_9 was applied twice per week to the soil. **A**) Plant height for these plants was measured over time. The following phenotypic characteristics were measured at the early pod stage of the plant: **B**) green mass and **C**) root mass. n = 7-9 per treatment with means ± SD shown. Statistical significance was determined using a two-way ANOVA and Dunnett's multiple comparison test, with the GA^+ water treatment used as the control. For height measurements in panel **A**, statistical significance was only assessed between treatments within a single time point. n.s. = not significnt ($p > 0.05$). In panel "a", if no p value is given, then the experimental group has a p value > 0.05.

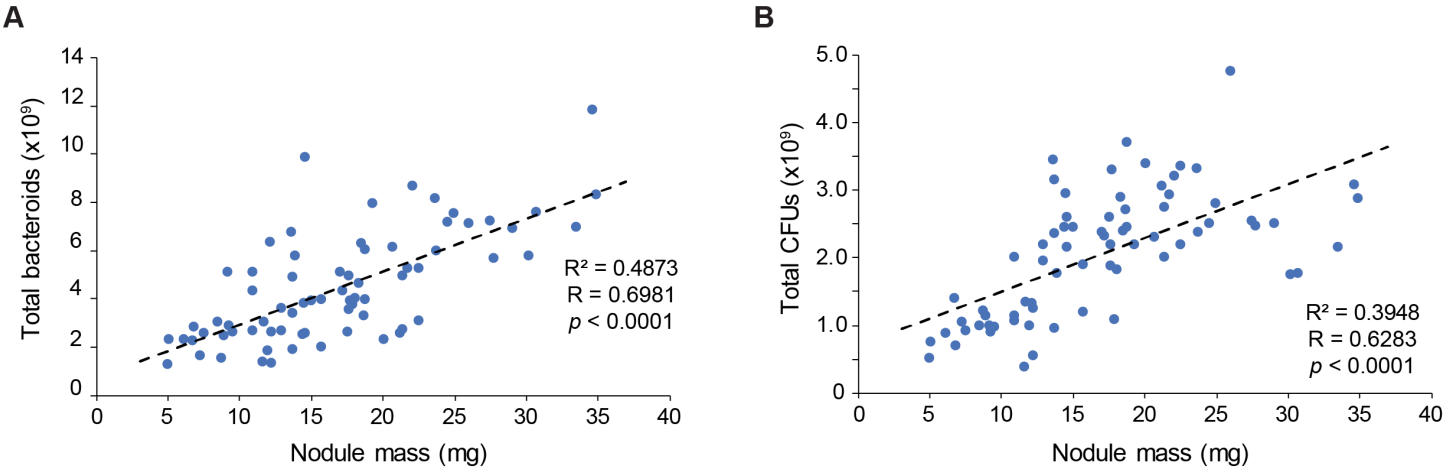

Supplementary Figure 17. Correlations between nodule size and bacteroid numbers. A) Total bacteroid cells extracted from nodules of varying sizes, as counted with flow cytometry, in relation to the mass of the nodule from which they were isolated. **B**) The total number of viable cells in the same samples was determined by plating for colony-forming units (CFUs). Data sets were analyzed in JMP Pro 13 to obtain statistical parameters of linear regressions.

Supplementary Table 1. Bacterial strains used in this study.

Strain	Description	Source
One Shot® TOP10 Chemically Competent *E. coli*	F- *mcrA, Δ(mrr-hsdRMS-mcrBC), Φ80lacZΔM15, Δ lacX74, recA1, araD139, Δ(araleu)7697, galU, galK, rpsL(StrR), endA1, nupG;* for plasmid propagation and cloning	Thermo Fisher Scientific
One Shot® BL21 Star™ (DE3) Chemically Competent *E. coli*	F- *ompT hsdSB (rB-, mB-) galdcmrne131* (DE3); for pET101 expression of soybean GA 3-oxidases	Thermo Fisher Scientific
E. coli S17-1 λ *pir*	F-, *RP4-2(Km::Tn7,Tc::Mu-1)*, *pro-82*, *LAMpir*, *recA1*, *endA1*, *thiE1*, *hsdR17*, *creC510*; for creating the *B. diazoefficiens* insertional mutant strain *Bd*KB2011	[2]
Bradyrhizobium diazoefficiens USDA 110 (*Bd*USDA110, formerly *B. japonicum* USDA 110,)	wild-type rhizobial symbiont of *Glycine max;* Cm^R, Tm^R	USDA; Beltsville, MD
B. diazoefficiens KB2011 (*Bd*KB2011)	*B. diazoefficiens* USDA 110 derived strain containing an insertion in *cyp112* for disruption of the entire GA operon	This study
BdΔcyp117	*cyp117* deletion strain derived from *B. diazoefficiens* USDA 110 parent strain; Cm^R	[3]
BdΔcyp114	*cyp114* deletion strain derived from *B. diazoefficiens* USDA 110 parent strain; Cm^R	[3]

Supplementary Table 2. Primers used in this study**.** Restriction sites are indicated with underlined nucleotide sequence. bp = base pairs, kb = kilobase.

Primer	Sequence (5' to 3')	Description
For cloning synthetic soybean GA 3-oxidases		
GmGA3ox4 F	CACCATGGTTACCACAC TGAGCGAAG	Forward primer for amplifying synthetic GmGA3ox4. Contains a 5' CACC for cloning into pET101/D-TOPO.
GmGA3ox4 R	TTAGTTATTATTCAGCA TGCTAATCAGGC	Reverse primer for amplifying synthetic GmGA3ox4. Contains the native stop codon to prevent the addition of a His tag in pET101/D-TOPO.
GmGA3ox6 F	CACCATGGCAACCAC ACTGAGCGAAG	Forward primer for amplifying synthetic GmGA3ox6. Contains a 5' CACC for cloning into pET101/D-TOPO.
GmGA3ox6 R	TTAGTTTTTCAGCAT GCTAATCAGGCTC	Reverse primer for amplifying synthetic GmGA3ox6. Contains the native stop codon to prevent the addition of a His tag in pET101/D-TOPO.
For amplifying a fragment containing cyp112 and flanking sequences for creation of the B. diazoefficiens KB2011 insertional mutant		
Bd-cyp112-PmeI-F	CCACGTTTAAACTCG AACCTCCTTCACCAAT CCGTA	Forward primer upstream of *cyp112*. Contains PmeI restriction site at the 5' end.
Bd-cyp112-PmeI-R	CTCCGTTTAAACTGTC GATCTGGCCCATGGT GAAAT	Reverse primer downstream of *cyp112*. Contains PmeI restriction site at the 5' end.
For confirming insertion within cyp112 in B. diazoefficiens KB2011		
Bd-CYP112-kb F	TGGTGGGTGACAGGCT ATGACGAGG	Forward primer 5' to the ~2 kb cassette insertion site in *cyp112*.

		Wild-type amplicon = 762 bp; insertion mutant = 2.8 kb
Bd-CYP112-kb R	TCACGTCGGTCCTCGGA TAGCGCATG	Reverse primer 3' to the ~2 kb cassette insertion site in *cyp112*. Wild-type amplicon = 762 bp; insertion mutant = 2.8 kb
For confirming clean deletion strains of B. diazoefficiens USDA 110		
Bd-CYP117ko-check F	ATCGTCAACATGTCGTC GTGCCAGG	Forward primer ~400 bp upstream of *cyp117* to check for presence or deletion of this gene; wild-type fragment = 2.1 kb, knockout = 0.8 kb
Bd-CYP117ko-check R	TGCGCCGGCAGCCAAA CAGAGC AAG	Reverse primer ~400 bp downstream of cyp117 to check for presence or deletion of this gene; wild-type fragment = 2.1 kb, knockout = 0.8 kb
Bd-CYP114ko-check F	ATTCCCGCGGAGAGCA AGGTGC	Forward primer ~400 bp upstream of *cyp114* to check for presence or deletion of this gene; wild-type fragment = 2.2 kb, knockout = 0.8 kb
Bd-CYP114ko-check R	ATAGCCGCCGAGCCATC AATGT CGGC	Reverse primer ~400 bp downstream of *cyp114* to check for presence or deletion of this gene; wild-type fragment = 2.2 kb, knockout = 0.8 kb
To amplify fragments for use as templates in determining qPCR primer efficiency		
BdCYP112 frag-F	TGGTGGGTGACAGGCT ATGACGAGG	Forward primer; amplicon = ~ 800 bp
BdCYP112 frag-R	TCACGTCGGTCCTCGGA TAGCGCATG	Reverse primer; amplicon = ~ 800 bp
BdKS frag-F	ATGATCCAGACTGAAC GCGCGGTG	Forward primer; amplicon = 831 bp
BdKS frag-R	TGGTCGAGGTCCGGTAG TACTGC	Reverse primer; amplicon = 831 bp
BdhisS frag-F	ACCCCAGAAACTGAAG GCGCGCCTG	Forward primer; amplicon = 1.5 kb

BdhisS frag-R	CTAGCCCCAGCTCACGTCATGGC	Reverse primer; amplicon = 1.5 kb
GmGA3ox4 frag-F	ATGCATGGCCTCAATCTGAAGATGG	Forward primer; amplicon = 863 bp
GmGA3ox4 frag-R	TCAAGGAACGAAACCGAGGCAAGG	Reverse primer; amplicon = 863 bp
GmGA3ox6 frag-F	TTCACTTAGGACCTTACCTGATTCG	Forward primer; amplicon = 877 bp
GmGA3ox6 frag-R	AATCAAGAACCAAAGGAGAAACCAC	Reverse primer; amplicon = 877 bp
cons7 frag-F	AGTCTCCTGGTAACATTGAGCAAAG	Forward primer; amplicon = 540 bp
cons7 frag-R	ATGAGAGTGCCCAATATTACAGGTG	Reverse primer; amplicon = 540 bp

To check for expression of the 6 GA3ox isoforms in soybean

GmGA3ox1 check-F	ACTGTCAACCCAATGATGATGCATC	Forward primer; amplicon = 796 bp after splicing of an intron from the gene
GmGA3ox1 check-R	CATCGGTGGAGAATAGAAATAAGCC	Reverse primer; amplicon = 796 bp after splicing of an intron from the gene
GmGA3ox2 check-F	ATGGTCTCACTCTCAACCCAACGATG	Forward primer; amplicon = 851 bp after splicing of an intron from the gene
GmGA3ox2 check-R	ACAGAGTCAACTAAAGGAGAAACC	Reverse primer; amplicon = 851 bp after splicing of an intron from the gene
GmGA3ox3 check-F	ACACAAGCACCCTGACTTAAACTCC	Forward primer; amplicon = 952 bp after splicing of an intron from the gene
GmGA3ox3 check-R	TGCCAAGGTACTCATTCCAAGTCAC	Reverse primer; amplicon = 952 bp after splicing of an intron from the gene

GmGA3ox4 check-F	ATGCATGGCCTCAATCT GAAGATGG	Forward primer; amplicon = 863 bp after splicing of an intron from the gene
GmGA3ox4 check-R	TCAAGGAACGAAACCG AGGCAAGG	Reverse primer; amplicon = 863 bp after splicing of an intron from the gene
GmGA3ox5 check-F	AGTCTTACACTTGGACA CACCATGG	Forward primer; amplicon = 909 bp after splicing of an intron from the gene
GmGA3ox5 check-R	AGGTACTCATTCCAAGT CACTGCC	Reverse primer; amplicon = 909 bp after splicing of an intron from the gene
GmGA3ox6 check-F	TTCACTTAGGACCTTAC CTGATTCG	Forward primer; amplicon = 877 bp after splicing of an intron from the gene
GmGA3ox6 check-R	AATCAAGAACCAAAGG AGAAACCAC	Reverse primer; amplicon = 877 bp after splicing of an intron from the gene

Supplementary Table 3. Plasmids and expression constructs used in this study.

Plasmid/construct	Description	Source
Plasmids		
pCR™-Blunt II-TOPO®	For cloning and propagation of blunt-end PCR constructs; Km^R	Thermo Fisher Scientific
pET101/D-TOPO®	For directional cloning and expression; contains C-terminal His-tag; Cb^R	Thermo Fisher Scientific
pJET	For cloning of the DNA fragments from *B. diazoefficiens* used to create the insertional mutant *Bd*KB2011; Cb^R	Thermo Fisher Scientific
pLO1	Mobilizable, mating/SacB counterselection vector; Km^R	[4]
pLOBJ3	pLO1 containing the GA operon knockout cassette used to created the insertional knockout strain *Bd*KB2011; Km^R	This study
Expression constructs		
pET101-sGmGA3ox4	For expression of synthetic soybean GA3ox4 in *E. coli*; Cb^R	This study
pET101-sGmGA3ox6	For expression of synthetic soybean GA3ox6 in *E. coli*; Cb^R	This study

Supplementary Table 4. Primers used for qPCR for selected *Bradyrhizobium diazoefficiens* USDA 110 and soybean (*Glycine max* cv. Williams ’82) gene transcripts.

target	forward primer (5’-3’)	reverse primer (5’-3’)	amplicon size (bp)
B. diazoefficiens genes			
cyp112	ATCGAATTCGGCCTGCTA	AGGATTTCCTCTACCGCCTT	97
sdr	CATGCTGTCGTCCTCACTTG	GAGGAGTCGCTCGGTCAT	94
ks	CTACGCGAACGTGTTCTGTT	CAAGGTCGCCATATCCAGC	64
hisS	GATGGAATACACCGACGCGCT	AACGCAAGCTAATCCACTGCTCG	106
G. max genes			
GmGA3ox4	ATCTGGCATAATGACTGTGC	GTTGGTTGAACCAATCCACC	150
GmGA3ox6	TCCATGTGATGATGCCAAAAAG	TTTTGCTCCTCAGAAATGCCC	150
cons7	ATGAATGACGGTTCCCATGTA	AGCATTAAGGCAGCTCACTCT	114

SUPPLEMENTARY REFERENCES

1. Prentki P, Krisch HM. In vitro insertional mutagenesis with a selectable DNA fragment. *Gene* 1984; **29**: 303–313.
2. de Lorenzo V, Eltis L, Kessler B, Timmis KN. Analysis of *Pseudomonas* gene products using *lacI*^{q}*/Ptrp-lac* plasmids and transposons that confer conditional phenotypes. *Gene* 1993; **123**: 17–24.
3. Nett RS, Montanares M, Marcassa A, Lu X, Nagel R, Charles TC, et al. Elucidation of gibberellin biosynthesis in bacteria reveals convergent evolution. *Nat Chem Biol* 2017; **13**: 69–74.
4. Lenz O, Schwartz E, Dernedde J. The *Alcaligenes eutrophus* H16 *hoxX* gene participates in hydrogenase regulation. *J Bacteriol* 1994; **176**: 4385–4393.